JCB Journal of Cell Biology

ARTICLE

Melanoma cells repress Desmoglein 1 in keratinocytes to promote tumor cell migration

Hope E. Burks[1], Jenny L. Pokorny[1], Jennifer L. Koetsier[1], Quinn R. Roth-Carter[1], Christopher R. Arnette[1], Pedram Gerami[1,2,3], John T. Seykora[4], Jodi L. Johnson[1,2], Ziyou Ren[1,2,3], and Kathleen J. Green[1,2,3]

Melanoma is an aggressive cancer typically arising from transformation of melanocytes residing in the basal layer of the epidermis, where they are in direct contact with surrounding keratinocytes. The role of keratinocytes in shaping the melanoma tumor microenvironment remains understudied. We previously showed that temporary loss of the keratinocyte-specific cadherin, Desmoglein 1 (Dsg1), controls paracrine signaling between normal melanocytes and keratinocytes to stimulate the protective tanning response. Here, we provide evidence that melanoma cells hijack this intercellular communication by secreting factors that keep Dsg1 expression low in the surrounding keratinocytes, which in turn generate their own paracrine signals that enhance melanoma spread through CXCL1/CXCR2 signaling. Evidence suggests a model whereby paracrine signaling from melanoma cells increases levels of the transcriptional repressor Slug, and consequently decreases expression of the Dsg1 transcriptional activator Grhl1. Together, these data support the idea that paracrine crosstalk between melanoma cells and keratinocytes resulting in chronic keratinocyte Dsg1 reduction contributes to melanoma cell movement associated with tumor progression.

Introduction

Cutaneous melanoma is a deadly skin cancer arising from pigmented melanocytes within the epidermis. Interactions between melanoma cells and their surrounding microenvironment play a critical role in tumor initiation and progression (Brandner and Haass, 2013; Villanueva and Herlyn, 2008; Wang et al., 2016). Discoveries surrounding immune cell interactions in solid tumors have led to significant innovation in clinical treatment strategies across multiple malignancies, including melanoma (Kalaora et al., 2022). Similarly, fibroblast–melanoma cell interactions have been established as important contributors to melanoma spread within the dermis (Galbo et al., 2021). However, less is known about how communication between melanocytes and their more abundant keratinocyte neighbors promotes melanoma development or initial stages of melanoma movement within and away from the epidermal environment.

It is well known that melanocyte–keratinocyte communication is crucial for mediating protective responses to ultraviolet radiation (UV; Upadhyay et al., 2021; Wang et al., 2016; Yardman-Frank and Fisher, 2021). UV elicits a cascade of signaling between the two cell types, resulting in the production of melanin by melanocytes, which is transferred to keratinocytes, where the pigment is positioned over the nucleus to protect the DNA from UV-mediated damage. Changes in communication between pigmented cells and keratinocytes continuously evolve in the developing melanoma environment (Brandner and Haass, 2013). Melanoma cells can escape control by adjacent keratinocytes by losing their intercellular contacts, allowing uncontrolled proliferation and spread (Wang et al., 2016). Primary melanomas are distinguished histologically by two growth phases: radial growth phase, characterized by intraepidermal proliferation and spread, and vertical growth phase, characterized by invasion into the dermis with the potential for metastasis. While some vertical growth phase melanomas arise de novo, they can also develop from radial growth phase lesions (Crowson et al., 2006). Cell contact between radially spreading melanoma cells and differentiated keratinocytes can then trigger vertical growth through Notch signaling, promoting movement of melanoma cells into the dermis (Golan et al., 2015). Major contributors to cell contact–mediated communication between keratinocytes and melanocytes are members of the cadherin family of cell–cell adhesion molecules. For instance, loss of E-cadherin (Ecad) is associated with the loss of keratinocyte

[1]Department of Pathology, Feinberg School of Medicine, Northwestern University, Chicago, IL, USA; [2]Department of Dermatology, Feinberg School of Medicine, Northwestern University, Chicago, IL, USA; [3]Robert H. Lurie Comprehensive Cancer Center, Northwestern University, Chicago, IL, USA; [4]Department of Dermatology, Perelman School of Medicine at the University of Pennsylvania, Philadelphia, PA, USA.

Correspondence to Kathleen J. Green: kgreen@northwestern.edu.

control over melanoma cell proliferation and invasion (Haass et al., 2005; Hsu et al., 2000). Further, increased P-cadherin stabilizes heterotypic adhesions between keratinocytes and melanoma cells to promote melanoma cell expansion and is associated with reduced survival in humans (Mescher et al., 2017).

Beyond cadherins' functions in direct contact, a role for vertebrate-specific cadherins known as desmogleins in paracrine signaling has recently emerged. Desmogleins work with partner desmocollin proteins to make up the adhesive core of desmosomes, essential intercellular junctions that provide structural integrity to the skin and are critical for epidermal barrier function (Hegazy et al., 2022; Kowalczyk and Green, 2013). Desmoglein 1 (Dsg1) is a keratinocyte-specific desmosomal cadherin found in complex stratified tissues of terrestrial organisms (Green et al., 2020). Work in our lab has shown that Dsg1 plays roles in cell signaling independent of its role as an adhesion molecule. Dsg1 promotes keratinocyte differentiation through suppression of EGFR-MAPK signaling by associating with Erbin, ultimately inhibiting Ras–Raf complex formation upstream of ERK1/2 to promote differentiation (Harmon et al., 2013). Dsg1 also controls cytokine signaling to dampen inflammation, and its loss in patients with biallelic mutations in Dsg1 results in the inflammatory condition severe dermatitis, multiple allergies, and metabolic wasting (SAM) syndrome (Godsel et al., 2022; Polivka et al., 2018; Samuelov et al., 2013).

We recently showed that paracrine signaling controlled by keratinocyte Dsg1 also controls melanocyte behavior (Arnette et al., 2020). Dsg1, but not Ecad, is temporarily lost in a dose-dependent manner following acute UV radiation (Johnson et al., 2014). Modeling this behavior, genetic interference resulting in acute loss of Dsg1 affects melanocyte pigmentation and dendricity in a manner reminiscent of the tanning response through secretion of a subset of cytokines also known to be generated in keratinocytes stimulated with UV (Arnette et al., 2020). While acute loss of Dsg1 seems to play a protective role in the skin by activating the tanning response, long-term loss of keratinocyte Dsg1 promotes behaviors in melanocytes that mimic a malignant phenotype, such as pagetoid movement, an upward intraepidermal spread of melanocytes, in 3D organotypic cultures (Arnette et al., 2020). These observations reveal a potential role for the loss of keratinocyte Dsg1 in initiating metastatic spread in the primary melanoma niche, specifically in intra-epidermal movement, an understudied phenomenon in melanoma progression.

Here, through a combination of analyses of human melanoma tissues and in vitro mechanistic studies, we identify a bidirectional communication pathway between keratinocytes and melanoma cells. This communication depends on the melanoma cells' ability to reduce Dsg1 expression. Consequent keratinocyte-dependent paracrine stimulation of a neural crest-like signature in melanoma cells is associated with increased melanoma cell migration. Our data support the idea that melanoma cells reduce Dsg1 by producing paracrine factors that increase the activity of the transcription factor Slug and decrease levels of the Dsg1 transcription factor Grainyhead like 1 (Grhl1). The relevance of these changes is supported by analysis of human melanoma sections showing that persistent loss of Dsg1, but not Ecad, is associated with local melanoma spread, reduced Grhl1, and increased Slug. Based on these observations, we propose that melanomas hijack normal keratinocyte to melanocyte crosstalk to maintain a protumor environment.

Results

Dsg1 is reduced in melanoma-adjacent keratinocytes in the human epidermis

To address whether there is an association between Dsg1 loss and melanoma, benign and malignant melanocytic lesions were stained for Dsg1, Ecad in keratinocytes, and Melan-A (Mel-A) to mark melanoma cells (Fig. 1 A). Quantifying Dsg1 and Ecad border localization and staining intensity revealed that Dsg1 was significantly reduced in the keratinocytes directly adjacent to the Mel-A positive staining cells (melanocytes/melanoma cells) in melanoma samples compared with distant sites or control tissues (Fig. 1, B and C). In contrast, keratinocytes adjacent to melanocytes in benign nevi did not show any alteration in Dsg1 levels. Ecad staining remained unchanged in all conditions, demonstrating that the loss of Dsg1 is not solely attributable to a general loss of cell adhesion proteins in melanoma-adjacent keratinocytes (Fig. 1, D and E).

Melanoma cells downregulate keratinocyte Dsg1 through paracrine signaling

Comparisons of chronic sun-exposed skin and non-sun-exposed skin transcriptomes from the Genotype-Tissue Expression (GTEx) database showed no significant change in Dsg1 gene expression levels (Fig. S1 A). This, combined with our previous finding that Dsg1 levels recover over time after UV exposure (Johnson et al., 2014), suggests that sustained loss of Dsg1 is likely a disease-specific phenomenon and not the result of accumulated sun damage. Furthermore, Dsg1 is maintained in keratinocytes distant from lesional melanoma cells. This led us to ask whether keratinocyte Dsg1 is regulated by the adjacent melanoma cells.

To address this question, we began with a unidirectional approach using conditioned media from a panel of melanoma cell lines varying in growth phase and mutation status. Differentiated keratinocytes were cultured in conditioned media from control primary melanocytes or melanoma cell lines, and mRNA or protein was collected and assessed by RT-PCR or immunoblot, respectively. The mRNA and protein levels of Dsg1, but not Ecad or Desmoglein 3 (Dsg3), another desmosomal cadherin, were decreased in keratinocytes cultured in melanoma but not melanocyte-conditioned media (Fig. 2, A and B).

To address whether melanoma cells reduce keratinocyte Dsg1 expression in a physiologically relevant model of epidermal differentiation, keratinocytes and melanoma cells or melanocytes were cocultured for 6 or 10 d at an air-medium interface to stimulate keratinocyte stratification and differentiation. Of the lines tested, WM1341D cells formed discrete tumors along the basement membrane that facilitated accurate quantification of Dsg1 levels in the surrounding keratinocytes. In these 3D cultures, keratinocytes adjacent to melanoma cells, but not normal melanocytes, exhibited a significant decrease in Dsg1, but not

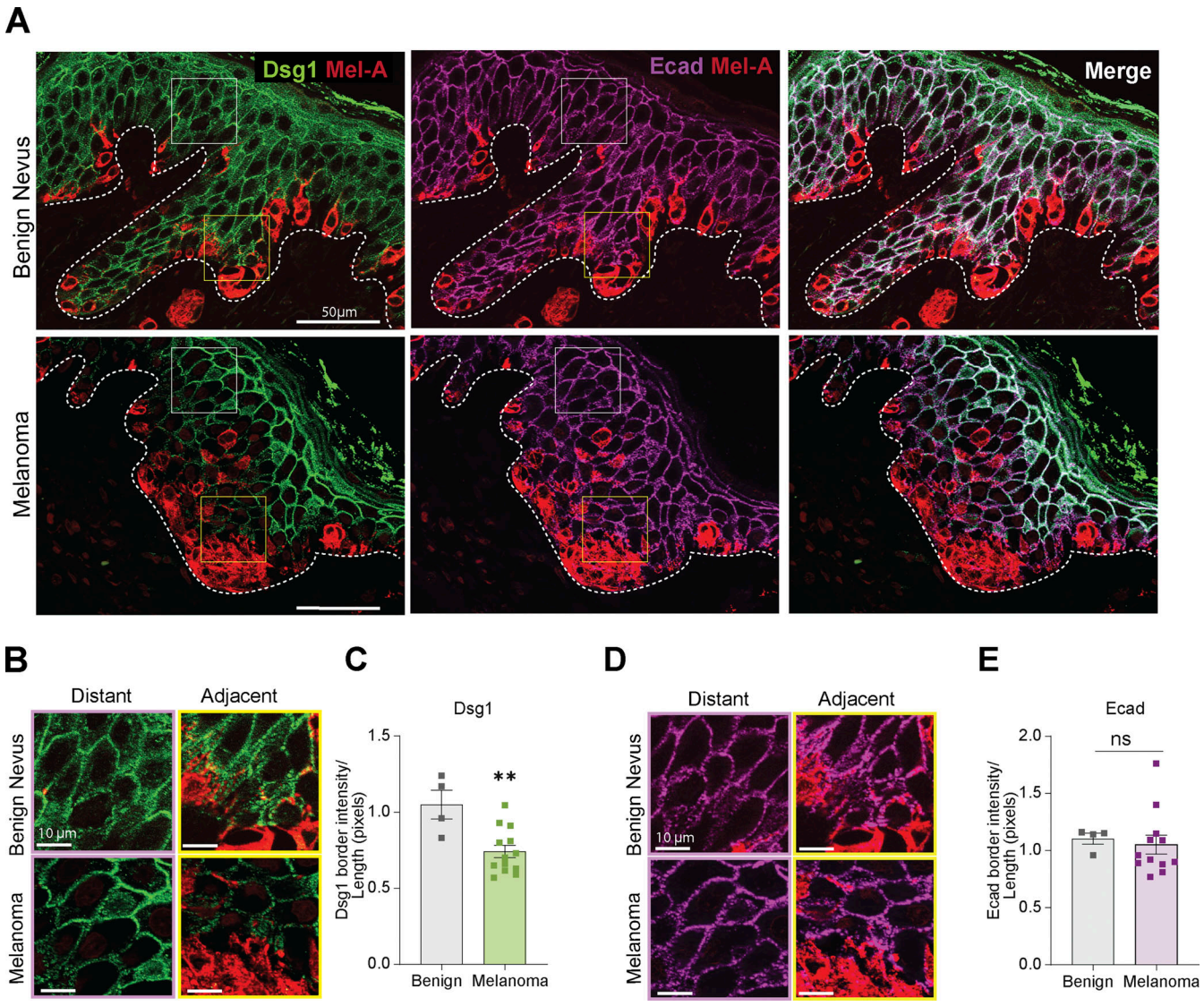

Figure 1. **Desmoglein 1 is reduced in melanoma-adjacent keratinocytes in human epidermis. (A)** Paraffin-embedded sections of benign nevi and primary-stage melanoma were costained for Dsg1 or Ecad and Mel-A to highlight cadherins at cell–cell interfaces of keratinocytes surrounding pigmented cells. The dashed line indicates basement membrane. **(B–E)** Both distant (two to four cells away) and proximal keratinocytes were examined for cadherin staining for quantification. Pixel intensities were determined for four benign and 12 melanoma samples and the ratio of proximal to distant intensities plotted. A significant decrease in Dsg1, but not Ecad, intensity proximal to the melanoma lesions was observed. (Note that the melanoma sample in the bottom panel was also used in Fig. 5 A where E-cadherin fluorescence intensity was correlated with the extent of melanoma cell spread.) Mean ± SEM depicted. **P < 0.01. Student's *t* test.

Ecad, at the cell borders, consistent with what was observed in patient melanoma lesions (Fig. 2, C and D). These data show that melanoma cells can downregulate Dsg1 transcription and protein in adjacent keratinocytes and support the idea that a secreted factor is, at least in part, responsible.

Transcriptomic analysis reveals increased activation of keratinocyte Slug and reduced keratinocyte differentiation signaling by melanoma cells

While keratinocyte Dsg1 is vital to the formation and maintenance of a functional epidermis, the mechanisms underlying its transcriptional regulation are poorly understood. To determine what pathways were altered in keratinocytes upstream and downstream of Dsg1 loss, we performed mRNA sequencing on keratinocytes that had been treated with melanoma or melanocyte-conditioned media. Two independent sequencing runs of identical samples (with biological $N = 3$) were performed as described in Materials and methods. A list of genes with fold changes for each run are included as Table S1. Data for Run #1 have been deposited to Github and data corresponding to Run #2 have been uploaded to GEO GSE239634. We utilized gene set enrichment analyses (GSEA) to analyze primary keratinocytes treated with melanoma-conditioned media from WM1341D or 501mel cells compared with keratinocytes treated with conditioned media from primary melanocytes using pathway data characterizing keratinocyte differentiation states in neonatal human skin (Fig. S1, B–G; Wang et al., 2020). These pathways were developed using primary human keratinocytes and were

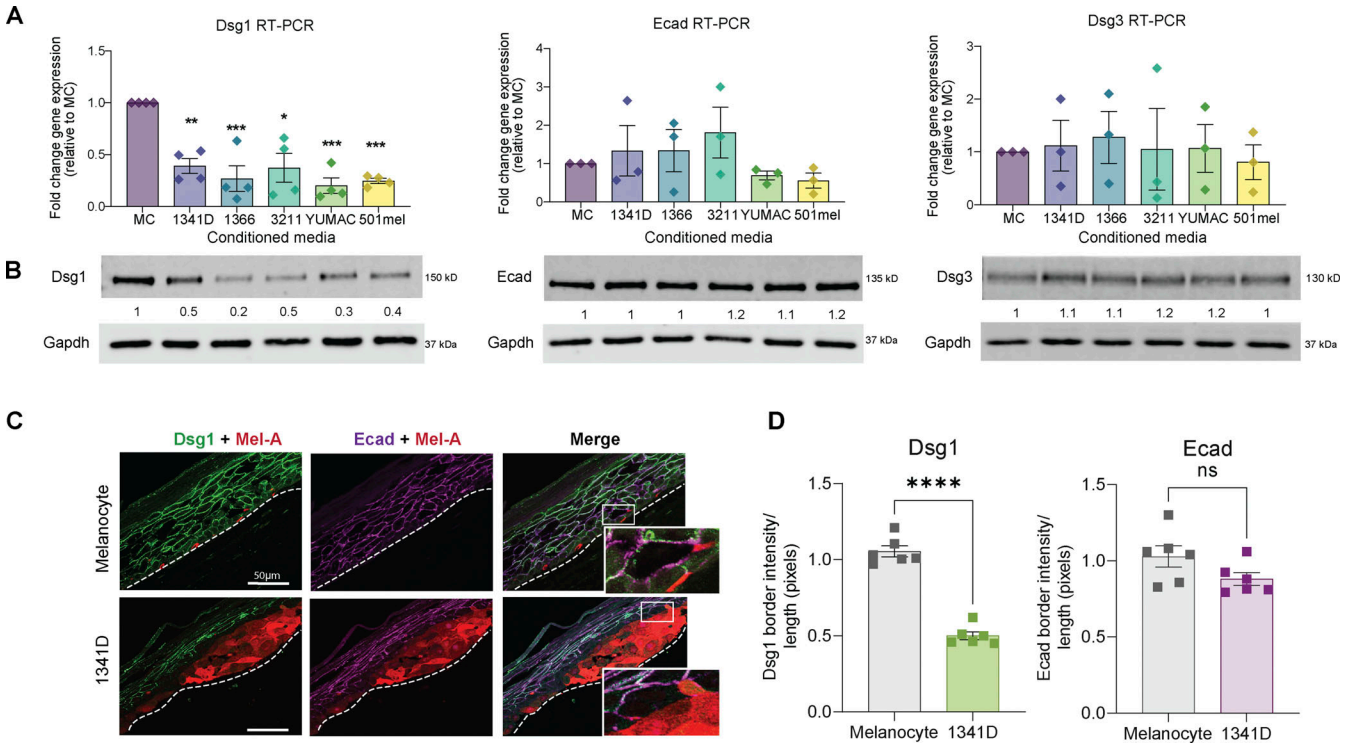

Figure 2. **Melanoma cells downregulate keratinocyte Dsg1 through paracrine signaling.** Primary human keratinocytes were treated for 24 h with conditioned media from melanocytes (MC) or the melanoma cell lines WM1341D (labeled as 1341D in figures), WM1366 (labeled as 1366 in figures), WM3211 (labeled as 3211 in figures), YUMAC, and 501mel, and RNA or protein was collected. **(A and B)** RT-PCR (A) and Western blots (B) were performed for Dsg1, Ecad, and Dsg3. Significantly lower mRNA and protein expression of Dsg1, but not Ecad or Dsg3, was observed. $n = 3$. Mean ± SEM depicted. *P < 0.05; **P < 0.01; ***P < 0.001. One-way ANOVA. **(C)** Melanocytes or WM1341D melanoma cells were seeded with normal primary keratinocytes and grown as 3D organotypic raft cocultures for up to 10 d. Paraffin sections were costained for Dsg1 or Ecad and Mel-A. The dashed line indicates the basement membrane. **(D)** Pixel intensities were determined and the ratio of proximal to distant intensities plotted. A significant decrease in Dsg1, but not Ecad, intensity proximal to the WM1341D lesions was observed. Mean ± SEM depicted. $n = 6$. *P < 0.05, Student's t test. Source data are available for this figure: SourceData F2.

thus chosen specifically for their relevance to our model system.

This analysis revealed a negative enrichment of gene sets characterizing the most differentiated keratinocyte states (granular and spinous) with some positive enrichment of more basal-like transcriptional states (Fig. S1, D–G). We previously showed that Dsg1 promotes keratinocyte differentiation through suppression of MAPK signaling. Consistent with this, upstream regulator analysis of our gene expression dataset using Ingenuity Pathway Analysis (IPA) predicted a significant increase in activation of MAPK signaling as indicated by increased ERK1/2 activation (Fig. S1 H). This prediction is consistent with our previous finding that the activation of MAPK signaling occurs downstream of Dsg1 loss to reduce keratinocyte differentiation.

The question remained as to what upstream factors stimulated by treatment with melanoma-conditioned media might regulate Dsg1 and the associated differentiation pathways. In this regard, another predicted upstream regulator that emerged was SNAI2 (Slug), which has been associated with stem-like properties of epidermal cells, as well as RAC1, which can activate Slug through PAK1 (Thaper et al., 2017; Yao et al., 2020). Slug can directly inhibit the expression of the transcription factor Grhl1, a transcriptional activator of Dsg1, and could mediate the negative enrichment of differentiated keratinocyte gene expression patterns (Mistry et al., 2014; Wilanowski et al., 2008). A potential role for keratinocyte Grhl1 in driving a permissive environment for melanoma progression has never been addressed.

Loss of Grhl1 and increased Slug are closely tied with melanoma-mediated Dsg1 loss

As Slug/Grhl1 signaling emerged as candidate regulators of Dsg1 from the RNA-Seq analysis, we set out to assess the extent to which a Slug/Grhl1/Dsg1 pathway is stimulated by paracrine signaling from melanoma cells (Fig. 3 A). Toward this end, we assessed Grhl1 mRNA and protein levels in keratinocytes treated with melanoma cell–conditioned media compared with those treated with melanocyte-conditioned media. Grhl1 mRNA and protein were downregulated by melanoma-conditioned media but remained unchanged in Dsg1-deficient keratinocytes compared with control, indicating that its loss is likely occurring upstream of melanoma-induced Dsg1 downregulation (Fig. 3, B and C; and Fig. S2, A and B). We also assessed the extent to which Grhl1 is decreased in keratinocytes adjacent to melanoma cells in 3D epidermal equivalent cultures (Fig. 3 D). As might be predicted from previous observations that Grhl1 is associated with the epidermal differentiation program, nuclear Grhl1 was present in a gradient in control cocultures, with the most intense

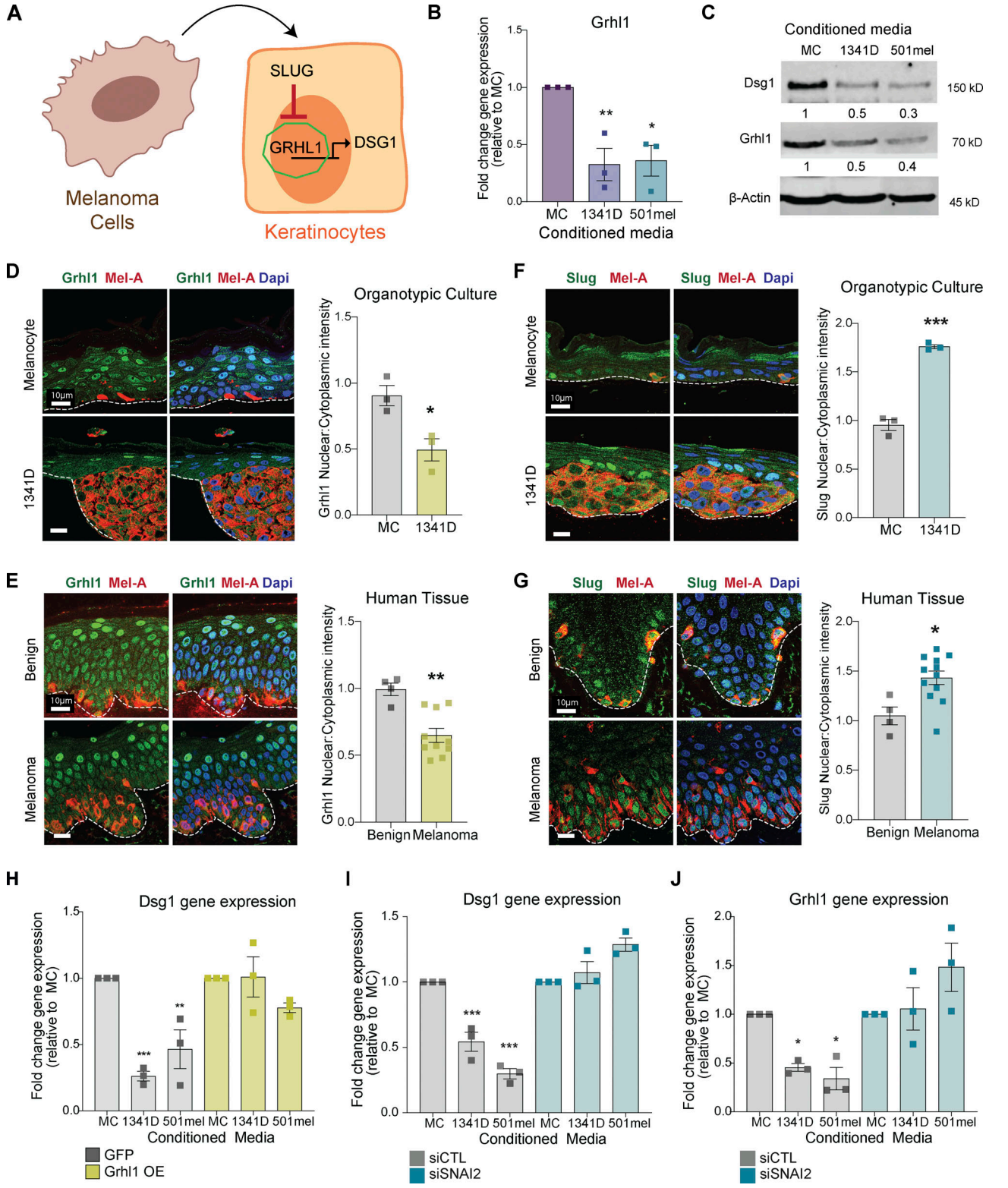

Figure 3. **Loss of Grhl1 is associated with melanoma-mediated Dsg1 loss. (A)** Model depicting the proposed signaling pathway leading to Dsg1 loss in keratinocytes. **(B and C)** Primary human keratinocytes were treated for 24 h with conditioned media from melanocytes (MC) or the melanoma cell lines WM1341D and 501mel and RNA or protein was collected. RT-PCR and Western blots were performed for Grhl1. Significantly lower mRNA and protein expression of Grhl1 was observed in the keratinocytes treated with melanoma-conditioned media when compared with melanocyte control–conditioned media. RNA levels and quantification for blots represent average fold change. Mean ± SEM depicted. $n = 3$. *P < 0.05, **P < 0.01, ***P < 0.001. One-way ANOVA. **(D)** Melanocytes or WM1341D melanoma cells were seeded with normal primary keratinocytes and grown as 3D organotypic raft cocultures for 6 d. Paraffin sections were costained for Grhl1 and Mel-A. Pixel intensities were determined and the ratio of proximal to distant intensities plotted. A significant decrease in Grhl1 intensity proximal to the WM1341D lesions was observed. Mean ± SEM *P < 0.05. Student's *t* test. **(E)** Paraffin-embedded sections of benign

nevi and melanomas were costained for Grhl1 and Mel-A and nuclear and cytoplasmic pixel intensities were measured in cells proximal to Mel-A stained cells and plotted as nuclear/cytoplasmic ratios. A significant decrease in keratinocyte Grhl1 intensity was observed in keratinocytes adjacent to melanoma compared with those in benign nevi. Mean ± SEM depicted. $n > 3$. **P < 0.01. Student's *t* test. **(F)** Melanocytes or WM1341D melanoma cells were seeded with primary keratinocytes and grown as 3D organotypic raft cocultures for 6–10 d. Paraffin sections were costained for Slug and Mel-A. Pixel intensities were determined, and the ratio of proximal to distant intensities was plotted. A significant increase in Slug intensity proximal to the WM1341D lesions was observed. $n = 3$ ±SEM; ***P < 0.001. Student's *t* test. **(G)** Paraffin-embedded sections of benign nevi and melanomas were costained for Slug and Mel-A. Nuclear and cytoplasmic pixel intensities were measured in cells proximal to Mel-A stained cells and the nuclear/cytoplasmic ratios were plotted. A significant increase in keratinocyte Slug intensity was observed in keratinocytes adjacent to melanoma compared with those in benign nevi. Mean ± SEM depicted. $n > 3$. *P < 0.05. Student's *t* test. **(H)** Primary human keratinocytes exogenously expressing GFP or Grhl1 were treated for 24 h with conditioned media from melanocytes (MC) or the melanoma cell lines WM1341D, and 501mel and RNA was collected. RT-PCR was performed for Dsg1. Introduction of Grhl1 into the keratinocytes rescued Dsg1 loss caused by melanoma conditioned media. $n = 3$. Mean ± SEM depicted. *P < 0.05; **P < 0.01; ***P < 0.001. One-way ANOVA. **(I and J)** Similarly, primary human keratinocytes exogenously expressing siCTL or siSNAI2 were treated for 24 h with conditioned media from melanocytes (MC) or the melanoma cell lines WM1341D, and 501mel and RNA was collected. RT-PCR was performed for Dsg1 and Grhl1. siSNAI2 transfected keratinocytes rescue Dsg1 and Grhl1 loss caused by melanoma-conditioned media. $n = 3$. Mean ± SEM depicted. *P < 0.05; **P < 0.01; ***P < 0.001. One-way ANOVA. Source data are available for this figure: SourceData F3.

nuclear staining present in the superficial, differentiated layers. Whereas Grhl1 was present in the most superficial layers of WM1341D cocultures, expression was significantly reduced in keratinocytes surrounding tumor cell clusters compared with control (Fig. 3 D). Similarly, keratinocytes surrounding melanoma cells in patient samples exhibited reduced Grhl1 staining compared with those surrounding melanocytes in benign nevi (Fig. 3 E). Grhl1 levels remained unchanged in Dsg1-deficient cultures compared with control in the 3D culture setting, further indicating that its loss likely occurs upstream of Dsg1 downregulation (Fig. S2 D). We next examined melanoma regulation of keratinocyte Slug using staining in 3D cultures. Slug exhibited a basal staining pattern in melanocyte-containing cultures, as is seen in normal human epidermal tissues. However, nuclear Slug levels were increased in suprabasal keratinocytes adjacent to WM1341D cells compared with keratinocytes two to four cells away from the melanoma cells (Fig. 3 F). Consistent with the decrease in Grhl1 staining in melanoma-adjacent keratinocytes, Slug staining was increased in lesional keratinocytes in clinical melanoma tumor sections (Fig. 3 G). We found no increase in suprabasal Slug staining in Dsg1 knockdown cultures compared with control, indicating that, like Grhl1, Slug is regulated by melanoma cells upstream of Dsg1 loss (Fig. S2 E).

Building upon these findings, analysis of a previously published dataset (Mistry et al., 2014) revealed that loss of Slug in primary human keratinocytes led to an increase in Dsg1 and Grhl1 gene expression with no change in Ecad, similar to what we see in keratinocytes in melanoma-conditioned media (Fig. S3 A). Furthermore, knockout of Slug in keratinocytes using siRNA leads to a concurrent increase in Dsg1 protein levels, supporting the role of Slug as a potential mediator of Dsg1 loss in melanoma-associated keratinocytes (Fig. S3 B).

To confirm the necessity of Slug activation and Grhl1 loss in melanoma-mediated downregulation of keratinocyte Dsg1, we first overexpressed Grhl1 or GFP control in keratinocytes and treated these cells with conditioned media from melanoma cells. GFP-expressing cells exhibited decreased Dsg1 transcription when treated with melanoma-conditioned media, but Dsg1 expression was largely retained in cells overexpressing Grhl1 under the same conditions (Fig. 3 H and Fig. S2 C). Similarly, siCTL (control) expressing keratinocytes exhibited a consistent decrease in Dsg1 gene expression when treated with melanoma-conditioned media, but their counterparts with SNAI2 knockdown did not show a change in Dsg1 expression (Fig. 3 I). Furthermore, the loss of Slug also abrogated the effect of melanoma-conditioned media on keratinocyte Grhl1, with SNAI2 knockdown cells showing no change in Grhl1 expression (Fig. 3 J and Fig. S3 C).

Together, these data support a model whereby melanoma cells mediate an increase in Slug and an accompanying decrease in Grhl1 and its downstream transcriptional target Dsg1 through paracrine signaling to keratinocytes (Fig. 3 A).

Loss of keratinocyte Dsg1 promotes melanoma cell migration in vitro and is associated with intraepidermal movement of melanoma cells in vivo

We next sought to identify the biological consequences of the loss of keratinocyte Dsg1 related to malignant behavior in melanoma cells. We performed RNA sequencing of melanoma cells treated with media from control or shDsg1 expressing keratinocytes followed by GSEA using previously published melanoma differentiation state signatures (Tsoi et al., 2018). This analysis revealed an enrichment in a neural crest-like signature in melanoma cells treated with Dsg1-deficient keratinocyte media (Fig. 4 A). We also observed a negative enrichment of the melanocytic signature, suggesting a general pattern of de-differentiation in these cells. Consistent with this, Gene Ontology (GO) pathway analysis revealed changes in mesoderm formation, negative regulation of cell differentiation, and regulation of EMT pathways, with increased expression of genes that have been linked to neural crest formation (Fig. 4 B). Among genes enriched in the melanoma cells treated with shDsg1 keratinocyte conditioned media were those related to extracellular matrix (ECM) and adhesion, including but not limited to collagens (COL2A1, COL4A3, and COL22A1 run 1 and 2), laminins (LAMC2, LAMB3, LAMB4 run 1; LAMA2 run 2), vitronectin (VTN) and syndecan 1 (SDC1; run1), NTN4 (run 2), as well genes encoding secreted factors linked to cell migration (e.g., IL-8, run 1 and WNT11, run 1 and 2; Table S1). Given that these signatures are associated with cell movement and migration, and that loss of keratinocyte Dsg1 leads to aberrant, pagetoid movement of melanocytes in 3D epidermal equivalents, we asked whether loss of Dsg1 in keratinocytes in turn promotes melanoma cell migration.

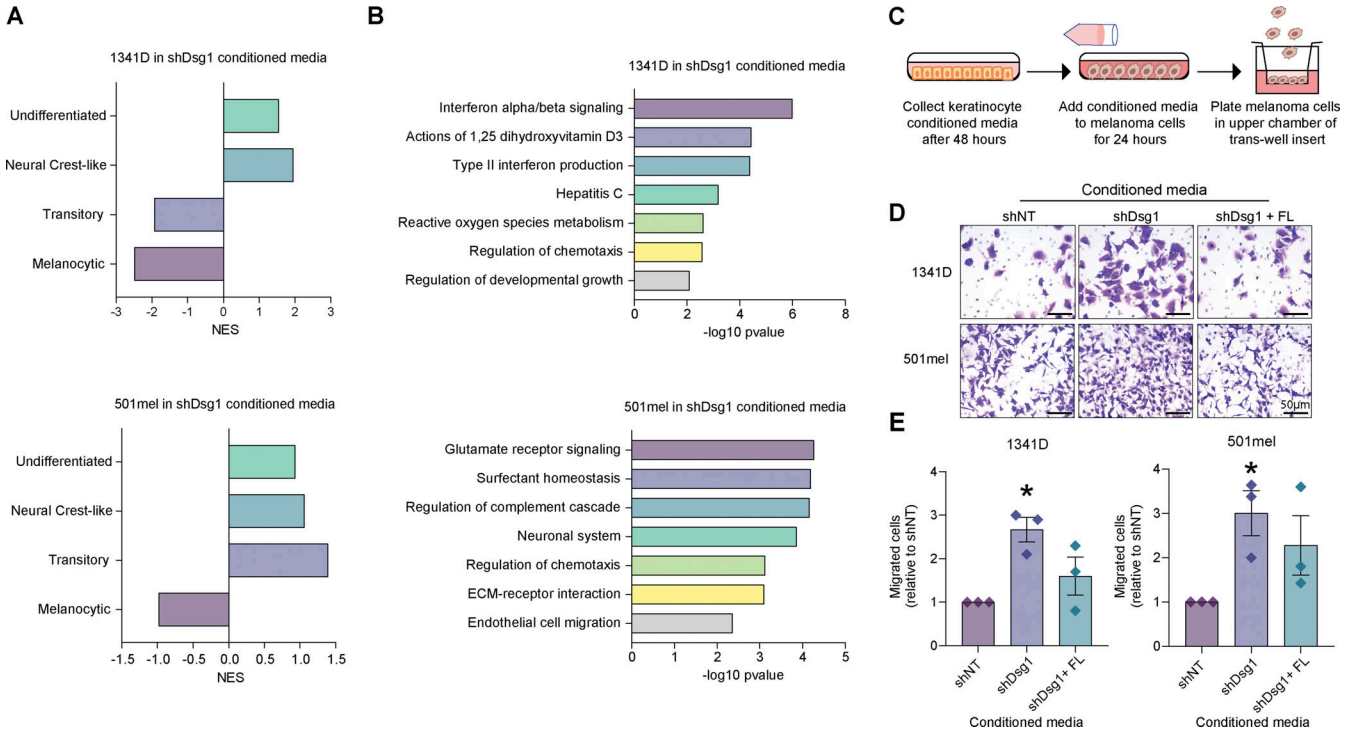

Figure 4. **Loss of keratinocyte Dsg1 drives melanoma cell migration.** Melanoma cells were cultured for 24 h in conditioned media from keratinocytes transduced with shNT or shDsg1 knockdown vectors and collected for RNA-sequencing. **(A and B)** GSEA comparing differentially expressed gene sets in RNA Seq run 2 to published signatures of melanoma signaling and differentiation. Normalized enrichment score (NES). **(B)** Top summary terms from Metascape for overrepresented in genes upregulated by shDsg1 keratinocyte conditioned media. **(C)** Schematic of trans-well migration assay. Melanoma cells were cultured in conditioned media from shNT expressing keratinocytes or shDsg1 expressing keratinocytes for 24 h. 50,000 cells were then seeded in serum-free media in the upper chamber of a trans-well insert (8- μM pore size). Lower wells contained DMEM supplemented with 5% FBS. **(D and E)** After 24 h, migrated cells were fixed and stained for visualization. Bars represent normalized migration compared with shNT control conditioned media. Mean ± SEM depicted. $n = 3$; *P <0.05 Student's t test.

To address this question, we cultured melanoma cells in conditioned media from keratinocytes expressing Dsg1 knockdown or control and then performed a trans-well migration assay (Fig. 4 C). Melanoma cells cultured in the Dsg1-deficient keratinocyte media showed increased levels of migration, while reintroduction of Dsg1 into deficient keratinocytes ameliorated this effect (Fig. 4, D and E). The fold change of melanoma cell migration exhibited a significant negative correlation with Dsg1 expression levels in keratinocytes with knockdown or rescue, with conditioned media from cells with the lowest Dsg1 resulting in the greatest fold change in migration (Fig. S4). These data support the idea that Dsg1 may be important for retaining melanoma cells in the primary tumor niche.

To investigate the relationship between keratinocyte Dsg1 and melanoma cell movement in vivo, we evaluated the extent to which melanoma spread in human patient samples was associated with Dsg1, Ecad, Grhl1, and Slug staining levels in surrounding keratinocytes. Notably, while we did see significant changes in melanoma-adjacent Dsg1, Grhl1, and Slug, we observed significant variability in the degree of change of each of these proteins. When we compared the levels of keratinocyte Dsg1 staining to the number of melanoma cells which had begun to move throughout the epidermis, we observed a significant negative correlation between keratinocyte Dsg1 and melanoma epidermal spread (Fig. 5, A and B). Keratinocyte Dsg1 was not correlated with the total number of melanoma cells in the lesions, indicating that the observed change in the number of migrating cells is likely not a result of increased cell number (Fig. 5 C). Consistent with this, there was no correlation between the number of melanoma cells in the niche and the number of cells moving throughout the epidermis.

A significant reciprocal association between Grhl1 and intraepidermal melanoma spread was also observed, while Slug showed a significant positive correlation (Fig. 5, A–C). While there is also variability in keratinocyte Ecad levels in melanoma lesions, we found no significant relationship between Ecad levels and melanoma cell number or melanoma cell movement. These data are consistent with the idea that the loss of keratinocyte Dsg1 and its upstream regulator Grhl1 play a role in the initial steps of melanoma cell movement and metastasis. Our data further suggest that paracrine signaling from melanoma cells may control the Dsg1/Grhl1 axis through activation of the repressor of keratinocyte differentiation gene SNAI2.

Melanoma cells increase ERK1/2 dependent keratinocyte production of CXCL1 downstream of Dsg1 loss to increase melanoma cell migration

We next investigated how the loss of Dsg1 in keratinocytes potentiates melanoma cell movement through paracrine signaling. Our previous work demonstrated that Dsg1-deficient

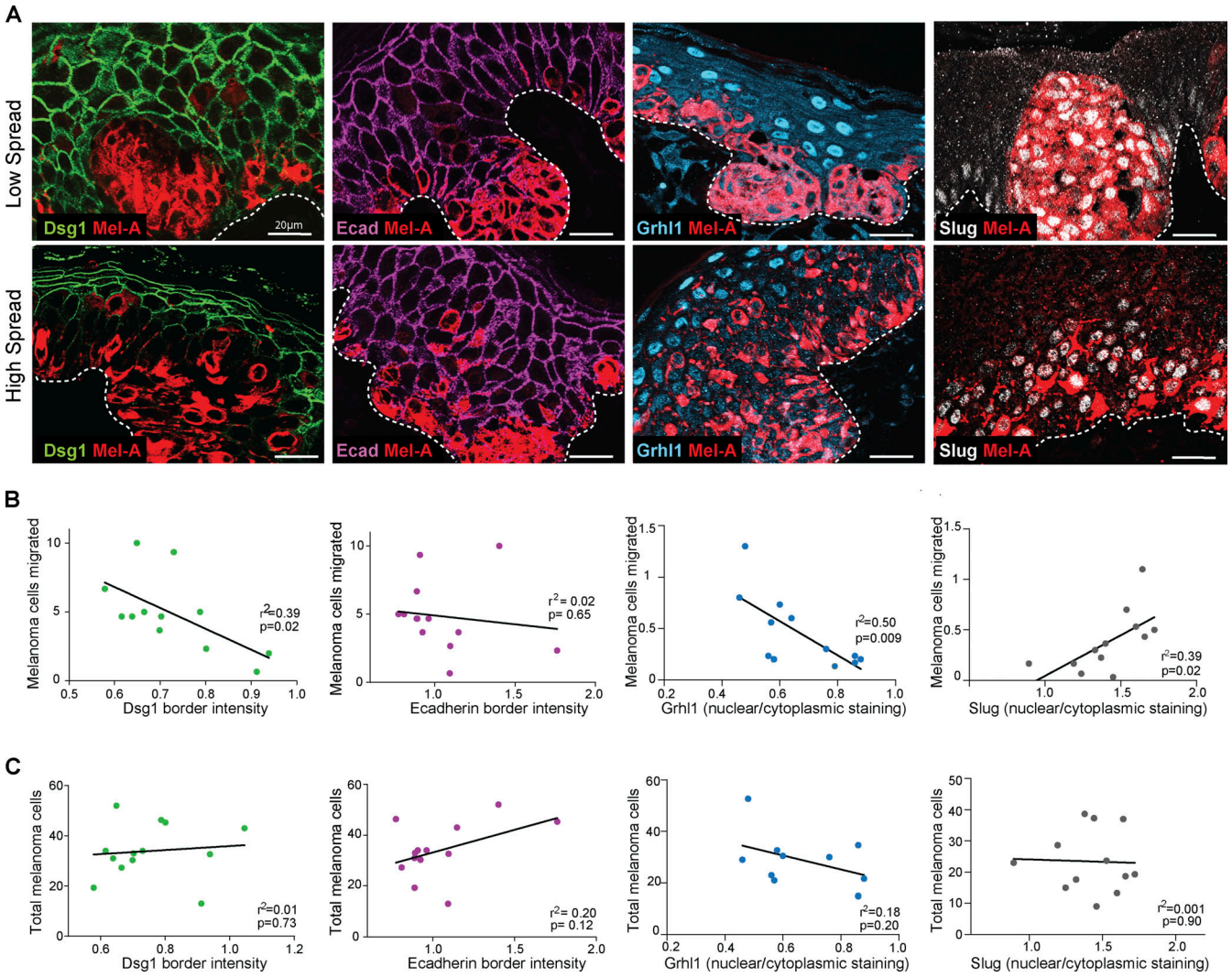

Figure 5. **Dsg1 and its regulators are associated with intraepidermal spread of melanoma cells in vivo. (A)** Paraffin-embedded sections of melanoma lesions were stained for Dsg1, Grhl1, Slug, or Ecad and Mel-A. **(B and C)** The number of individual melanoma cells spreading away from the basal layer, (B) as well as the total number of melanoma cells in each section (C) were counted and then correlated to the staining intensity of Dsg1, Grhl1, Slug, and Ecad. (Note that the E-cadherin/Mel-A stained tumor sample in the bottom panel was also used in Fig. 1 A for analysis of E-cadherin fluorescence intensity in proximal versus distal keratinocytes.) $n > 10$. Simple linear regression.

keratinocytes increase the secretion of inflammatory cytokines and chemokines, which are known to contribute to the formation and maintenance of the melanoma tumor niche. Chemokines previously identified as increased in the secretome of Dsg1-deficient keratinocytes include the GRO isoforms (CXCL1, CXCL2, and CXCL3) and IL-8, which bind the CXCR1 and 2 receptors, as well as the IL-6 cytokine (Arnette et al., 2020). To address whether keratinocytes grown in melanoma cell conditioned media exhibit increased chemokine expression like that seen with genetic knockdown of Dsg1, we assessed the gene expression levels of chemokines that bind the CXCR1 and CXCR2 receptors, as well as IL-6 in keratinocytes treated with media from WM1341D and 501mel cells. Of the secreted factors tested, we found that melanoma cells drive an increase in CXCL1 expression specifically in keratinocytes (Fig. 6 A and Fig. S5).

As mentioned above, upstream regulator analysis predicted an increase in ERK1/2 signaling, which can increase levels of CXCL1 (Cheng et al., 2019; Schweppe et al., 2006). Our previous work showed that genetic interference with Dsg1 results in increased ERK1/2 signaling. Indeed, when active p-ERK/total ERK was measured in keratinocytes grown in melanoma cell conditioned media, a significant increase was observed, like that which occurs in cells with genetic interference of Dsg1 (Fig. 6 B). To address whether the observed increase in CXCL1 depended on the ERK1/2 pathway, we treated cells in melanoma-conditioned media with the MEK1/2 inhibitor U0126. U0126 effectively reduced both ERK1/2 activation as well as CXCL1 gene expression (Fig. 6, C and D). Dsg1 levels are not rescued by ERK1/2 inhibition, indicating that melanoma-driven ERK1/2 signaling is likely downstream of and mediated by Dsg1 loss as indicated by our transcriptomic analysis.

CXCL1 exclusively binds to the CXCR2 receptor in melanoma cells. To confirm the role of CXCL1 in melanoma cell migration, we treated melanoma cells with a combination of keratinocyte-

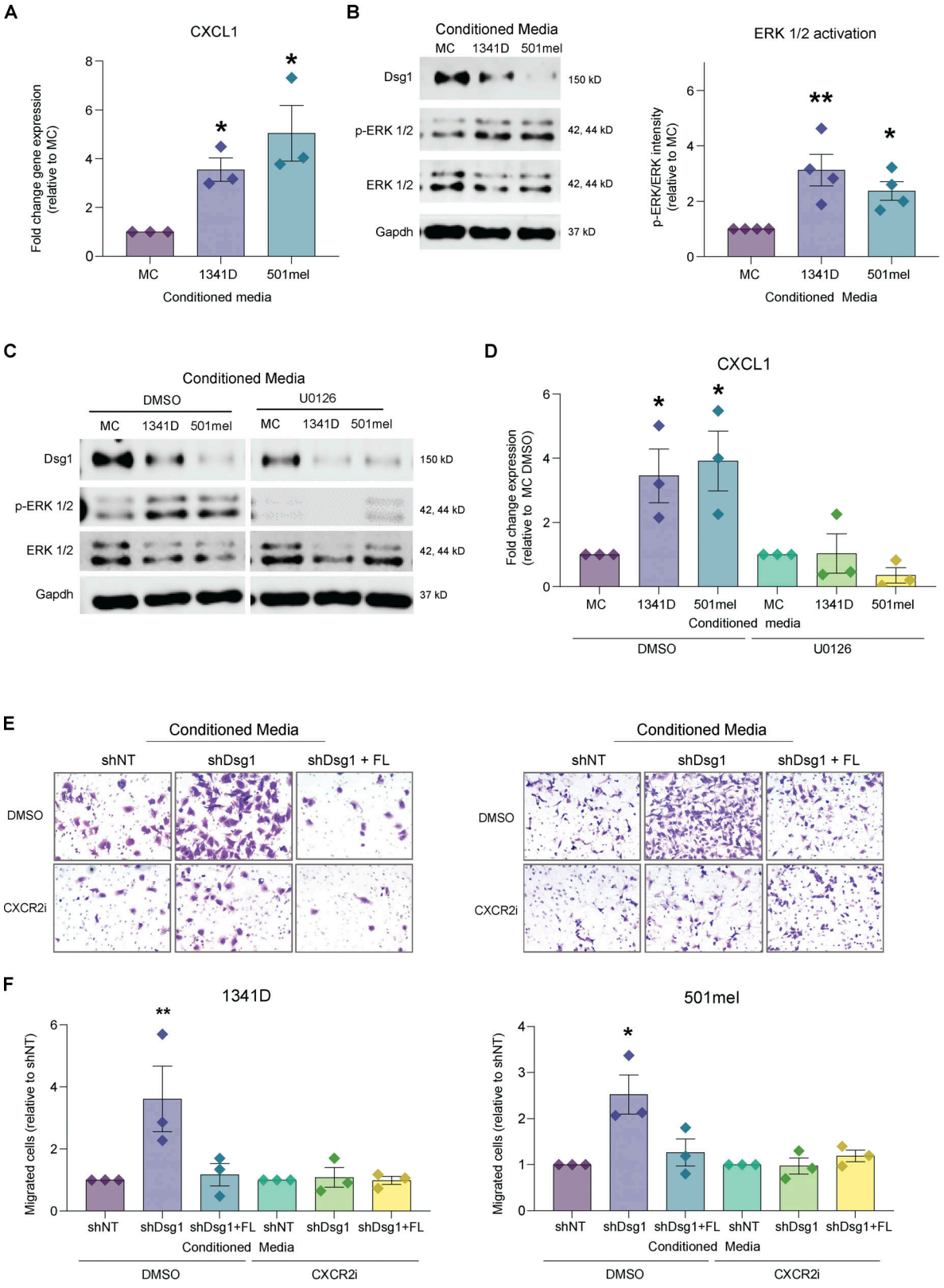

Figure 6. **Melanoma-induced loss of keratinocyte Dsg1 drives ERK1/2 dependent pro-migratory CXCL1 production. (A)** Primary human keratinocytes were treated for 48 h with conditioned media from melanocytes (MC) or the melanoma cell lines WM1341D and 501mel and RNA or protein was collected. RT-PCR was performed for CXCL1 expression. Mean ± SEM depicted. *n* = 3. *P <0.05. One-way ANOVA. **(B)** Western blot was performed for Dsg1, ERK1/2, and phosphor-ERK1/2. Mean ± SEM depicted. *n* = 4, *P <0.05 **P < 0.01. One-way ANOVA. Increased ERK1/2 phosphorylation was observed in keratinocytes treated with melanoma-conditioned media. **(C)** Primary human keratinocytes were treated with melanocyte or melanoma-conditioned media with either DMSO or 5 µM U0126 (MEK1/2 inhibitor). Western blot was performed to confirm a decrease in ERK1/2 phosphorylation in U0126-treated cells. *n* = 3.

(D) CXCL1 gene expression was no longer increased in keratinocytes treated with melanoma-conditioned media in the presence of U0126 $n = 3$. *P <0.05. One-way ANOVA. **(E and F)** Melanoma cells were treated with conditioned media from shNT, shDsg1, or shDsg1 plus a full-length (FL) wild-type Dsg1 rescue expressing keratinocytes for 24 h in the presence of DMSO or the CXCR2 inhibitor (500 nM SB22502) then plated for trans-well migration and collected after 24 h. Loss of keratinocyte Dsg1 no longer increased melanoma cell migration when the CXCL1 receptor, CXCR2, was inhibited. Mean ± SEM depicted. $n = 3$ *P < 0.05, **P < 0.01. One-way ANOVA. Source data are available for this figure: SourceData F6.

conditioned media and DMSO or the CXCR2 inhibitor SB225002. When the CXCL1 receptor CXCR2 was inhibited in melanoma cells, conditioned media from Dsg1-deficient keratinocytes was no longer able to induce migration, demonstrating a role for specific chemokine signaling in keratinocyte modulation of melanoma cell behavior (Fig. 6, E and F). Together these data highlight a novel mechanism of initiation of melanoma cell migration or increase of melanoma cell migration through direct manipulation of tumor niche keratinocytes.

Discussion

Melanoma is one of the most aggressive skin cancers due in part to its propensity to metastasize. The composition of the tumor microenvironment has an undeniably important influence on tumor cell behavior, including metastatic progression. Much of the work done investigating melanoma metastasis has been focused on cells once they have already escaped from the epidermis (Vandyck et al., 2021). Here, we examine the underappreciated role of keratinocytes in the initiation (or inhibition) of melanoma cell movement within the primary epidermal niche. Our work establishes a role for the keratinocyte-specific cadherin Dsg1 as a regulator of chemokine signaling whose loss is associated with cell spread in the melanoma tumor niche (Fig. 7). Furthermore, these studies shed light on the understudied mechanisms by which melanoma cells manipulate their epidermal microenvironment to facilitate metastatic progression.

Previous work has highlighted the importance of keratinocytes in restricting newly transforming melanocytes to their normal location in the basal epidermis. In particular, the role of cadherins in restricting the movement of melanoma cells has focused on their canonical roles in cell–cell adhesion. For instance, loss of Ecad, which is expressed in both keratinocytes and melanocytes, occurs in a progressive fashion in primary/invasive melanomas (Haass et al., 2005). Reintroduction of Ecad into Ecad-deficient melanoma cells inhibited invasion into the dermis of the 3D reconstructed epidermis through downregulation of invasion receptors MUC18 and β3 integrin (Hsu et al., 2000) and also impairs melanoma cell invasion in response to CXCL12 (Molina-Ortiz et al., 2009). The loss of Ecad in melanoma may also occur in concert with the upregulation of pro-migratory N-cadherin, possibly resulting in a cadherin switch similar to that reported for other tumors (Siret et al., 2015). Like Ecad, P-cadherin in the tumor environment promotes keratinocyte–melanoma cell contact. However, in this case, the interaction supports the expansion of melanoma cells and progression toward a more aggressive phenotype and poor survival in humans (Mescher et al., 2017). Overall, previous work on cadherins in melanoma progression has focused on the idea of permissive migration due to the removal of physical barriers or tumor progression due to cell contact-mediated signaling.

Here, we provide evidence for a novel paracrine function for the desmosomal cadherin, Dsg1, in shaping the early melanoma microenvironment. While playing an essential role in the physical barrier, Dsg1 has also emerged as a cell-autonomous regulator of signaling pathways that complement but do not depend on its physical role in adhesion (Arnette et al., 2020;

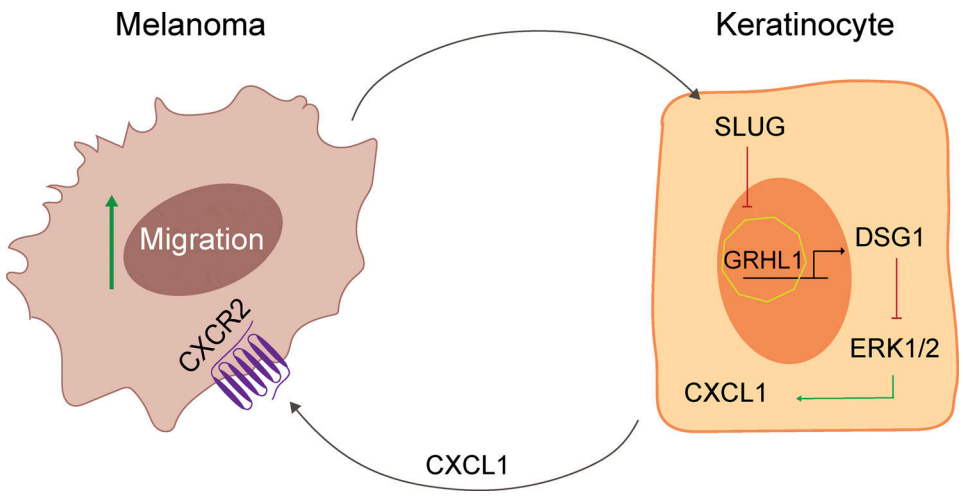

Figure 7. **Model: Bi-directional paracrine signaling between melanoma cells and keratinocytes potentiates melanoma cell movement.** Our data support a model whereby factors secreted from melanoma cells activate keratinocyte Slug, which in turn decreases Grhl1, a transcriptional activator of Dsg1. The consequent loss of Dsg1 activates ERK1/2 to increase keratinocyte CXCL1 production, which in turn promotes melanoma cell migration through activation of CXCR2.

Getsios et al., 2009; Harmon et al., 2013). Dsg1 loss due to genetic or environmental stimuli revealed a role in controlling differentiation and inflammation (Godsel et al., 2022). The data presented here add to Dsg1 functions and are consistent with a model whereby its loss in the context of melanoma drives melanoma cell migration. Changes in Dsg1 expression occur before any detectable decrease in Ecad, supporting the idea that these changes occur early in tumor development and that melanoma spread is not an indirect result of loss of this classic cadherin. Consistent with this, melanoma-conditioned media is sufficient to mediate a reduction in Dsg1 mRNA and protein in the absence of any significant changes in Ecad expression. While we have focused here on Dsg1's role in paracrine signaling between keratinocytes and melanoma cells, in vivo, these paracrine cues are likely to work in concert with cell contact-mediated signaling. Future studies will address the extent to which Dsg1 loss contributes to paracrine and cell contact–mediated pathways in melanoma progression.

Importantly, we have defined for the first time a potential transcriptional regulatory pathway co-opted by melanoma cells to reduce Dsg1 expression through Grhl1 and its upstream transcriptional repressor Slug. While Grhl1 has been shown to regulate epidermal homeostasis by controlling the differentiation program and barrier function (Wilanowski et al., 2008), a role in melanoma development has not been reported. Likewise, Slug has been linked to melanoma cell metastasis but not in the creation of a pro-melanoma keratinocyte compartment (Miao et al., 2021; Shirley et al., 2012). Slug is known to be expressed in the undifferentiated basal cell compartment of the epidermis and is important in the context of epidermal wound healing (Arnoux et al., 2008). Injury is also known to induce the expression of desmosome-associated stress-associated keratins like K6/16/17 that can alter desmoglein expression and function (Büchau et al., 2022). While transcripts encoding these keratins were unchanged in keratinocytes treated with melanoma-conditioned media, in the future, it will be worth more broadly considering how the desmosome-intermediate filament network controls the developing melanoma niche. Importantly, while increased Slug likely plays additional roles in shaping the early melanoma tumor environment, genetic targeting of Dsg1 is sufficient to initiate the signaling cascade that stimulates increased melanoma cell movement in vitro.

The factors in the melanoma media that cause this signaling cascade in the keratinocytes remain unknown. However, in addition to RAC1, our upstream regulator analysis also predicted an increased activation of ERK5, a kinase that has been implicated in the activation of Slug (Arnoux et al., 2008; Fig. S1), in keratinocytes treated with melanoma cell–conditioned media (run 1; run 2 501mel). In fact, there are many soluble proteins produced by melanoma cell lines such as growth factors (VEGF, EGF, and FGF2), which activate both ERK5 and RAC1 upstream of Slug. Melanoma cells have also been shown to communicate with surrounding cells through the production and release of exosomes. Delineating the specific messengers that manipulate keratinocytes in the melanoma microenvironment is an important endeavor moving forward.

Our observation that melanoma cells treated with conditioned media from Dsg1-deficient keratinocytes exhibit a neural crest-like signature is consistent with previous studies suggesting that malignant melanoma cells hijack the neural crest program to promote plasticity and facilitate invasion and metastasis (Diener and Sommer, 2021; Wessely et al., 2021). We further identify a CXCL1/CXCR2 axis as important for the increase in melanoma cell movement. CXCL1 signaling has been linked to stem cell phenotypes and tumor progression and invasion in other cancers (Tang et al., 2012; Wessely et al., 2021), and CXCR2 introduction into melanoma cells increases cell proliferation, motility, and invasion (Singh et al., 2009). CXCR2 may be more prevalent in late-stage melanomas and thus it will be important to explore other potential pathways in the early melanoma niche that could link Dsg1 reduction in keratinocytes to melanoma spread at the earliest stages (Sharma et al., 2010). Likewise, it will be important in the future to expand our studies to determine the potential role of Dsg1 loss in invasive spread through the basement membrane and into the dermis using physiologically relevant matrices.

Finally, here we uncovered novel paracrine regulation of melanoma behavior by the keratinocyte-specific molecule Dsg1. However, this cadherin also controls cell–cell adhesion and the mechanical properties of keratinocytes that along with paracrine signaling could impact melanoma behavior. In the future, understanding how both cell contact–mediated and paracrine signaling changes are integrated will be important for acquiring a cohesive understanding of factors shaping the tumor niche. Furthermore, the study of how the loss of Dsg1 contributes to the plasticity of the tumor cells, whether it stimulates migration of an existing rare population of melanoma cells or lowers the threshold for the emergence of a new population with neural crest features will be important for understanding the molecular mechanisms of communication between these two populations (Emert et al., 2021; Shaffer et al., 2017). As melanoma cells do not acquire new mutations (Shain et al., 2018) once they have left the epidermis, keratinocyte crosstalk could be a key shaper of melanoma behavior in the epidermal tumor niche. Changes in melanoma cells caused by a Dsg1-deficient microenvironment maintained over time could be targetable.

Materials and methods

Cell culture

Keratinocytes and melanocytes were isolated from discarded neonatal foreskin provided by the Northwestern University Skin Biology and Diseases Research-Based Center (NU-SBDRC; IRB #STU00009443) as previously described (Roth-Carter et al., 2022). Briefly, the foreskin was washed several times with PBS, excess fat and blood vessels were trimmed, and the tissue was cut into small pieces (~8 × ~8 mm) and placed in 2.4 U/ml of Dispase II (catalog no. 04942078001; Roche) diluted in PBS overnight at 4°C. The next day, the epidermis was removed and single cells were dissociated with 0.25% trypsin (catalog no. 25-050-CI; Corning) for 15 min at 37°C. FBS was added to inactivate the trypsin and the cells were split into two pools to collect keratinocytes using a 40-µm cell strainer or melanocytes using a 70-µm cell strainer.

Keratinocytes were grown in M154 medium (catalog no. M154CF500; Life Technologies) supplemented with human

keratinocyte growth supplement (catalog no. S-001-5; Life Technologies), 1,000× gentamycin/amphotericin B solution (catalog no. R01510; Life Technologies), and 0.07 mM $CaCl_2$. Confluent keratinocyte monolayers were differentiated in the media described with the addition of 1.2 mM $CaCl_2$. Melanocytes were cultured in Opti-MEM (catalog no. 11058-021; Life Technologies) containing 1% penicillin/streptomycin (catalog no. 30-002-CI; Corning), 5% fetal bovine serum (FBS; catalog no. F0926; Sigma-Aldrich), 10 ng/ml bFGF (catalog no. F1004; ConnStem Inc.), 1 ng/ml heparin (catalog no. H3393; Sigma-Aldrich), 0.1 mM N6, 2′-O-dibutyryladenosine 3:5-cyclic monophosphate (dbcAMP; catalog no. D0627; Sigma-Aldrich), and 0.1 mM 3-isobutyl-1-methyl xanthine (IBMX; catalog no. I5879; Sigma-Aldrich). Melanoma cells were cultured in DMEM containing sodium pyruvate (catalog no. 10-013-CV; Corning) with 1% penicillin/streptomycin, 5% FBS. WM1341D, WM1366, and WM3211 lines were purchased from Rockland Immunochemicals Inc. YUMAC and 501mel lines were kindly gifted by Jaehyuk Choi at Northwestern University. All cell lines were authenticated with DNA (STR) profiling and tested to rule out mycoplasma contamination.

Organotypic skin cultures

Organotypic cultures were grown as previously described (Arnette et al., 2016; Getsios et al., 2009) with the addition of melanocytes or melanoma cells co-seeded with keratinocytes at a 1:5 ratio to mimic the ratio seen in the basal layer of normal skin (Roth-Carter et al., 2022). Briefly, the organotypic cultures were generated by making collagen plugs containing J2 fibroblasts. Melanocytes or melanoma cells were then seeded on top of the collagen plug and left submerged for 1 d in their respective growth media. Keratinocytes were then added and the cultures were left submerged for an additional 2 d in E-Media. They then were lifted to an air–liquid interface and grown for an additional 6–10 d. Organotypic cultures fixed in 10% neutral buffered formalin (catalog no. HT501320; Sigma-Aldrich) were embedded in paraffin blocks and cut into 4-µm sections.

Preparation of conditioned media

Conditioned media from keratinocytes was prepared as previously described (Arnette et al., 2020). Briefly, keratinocytes were transduced with shNT, shDsg1, or shDsg1 plus silencing resistant Dsg1-Flag (FL) retroviruses. Once the cells reached confluence, the media was switched to 1.2 mM $CaCl_2$. After 3 d, fresh 1.2 mM $CaCl_2$ was added and the conditioned media was collected 2 d later. For melanocyte and melanoma conditioned media, cells were grown to 70–80% confluence in their respective growth media (see above), at which point the media was changed to DMEM containing sodium pyruvate (catalog no. 10-013-CV; Corning) with 1% penicillin/streptomycin, 5% FBS, and then collected after 72 h. Conditioned media was added to keratinocytes immediately upon collection.

Antibodies and reagents

The mouse monoclonal antibodies used were P124 (anti-Dsg1 extracellular domain; catalog no. 651111; Progen), anti-Dsg3 (5G11; catalog no. MABT335; EMD Millipore), 27B2 (anti-Dsg1 cytodomain; catalog no. 32-6000; Life Technologies), HMB45 (anti-Melanoma gp100; catalog no. MA5-13232; Thermo Fisher Scientific), and total ERK1/2 (catalog no. 4370S; Cell Signaling). The rabbit monoclonal antibody EP1576Y (anti-S100 beta; catalog no. ab52642; Abcam) was used. Rabbit polyclonal antibodies used were HECD1 (anti-E-cadherin; Takara), anti-Melan-A (catalog no. ab15468; Abcam), anti-GAPDH (glyceraldehyde-3-phosphate dehydrogenase; catalog no. G9545; Sigma-Aldrich), anti-GRHL1 (catalog no. PA5-31734; Thermo Fisher Scientific), anti-Slug (catalog no. 9585S; Cell Signaling), and anti-p-ERK (catalog no. 4370S; Cell Signaling). Secondary antibodies for immunoblotting were goat anti-mouse and goat anti-rabbit (LI-COR). Secondary antibodies for immunofluorescence were goat anti-mouse and goat-anti-rabbit linked to fluorophores of 488, 568, and 647 nm (Alexa Fluor; Life Technologies). DAPI (catalog no. 9542; Sigma-Aldrich) was used to stain nuclei. The MEK1/2 inhibitor (U0126) was purchased from Cell Signaling (catalog no. 9903S) and used at a 5 µM final concentration. The CXCR2 inhibitor (SB22502) was purchased from Selleck Chemicals (catalog no. S7651) and used at 500 nM final concentration.

DNA constructs and retroviral transduction

LZRS-shDsg1 (Dsg1shRNA), sequence LZRS-Dsg1 5′-TCGAAG TCGAATCACAAAGT-3′, and LZRS-Flag Dsg1 of NM_001942. 2 were generated as described (Getsios et al., 2004, 2009; Simpson et al., 2010). LZRS—NTshRNA was generated by inserting sequences NTshRNA-fwd 5′-GTATCTCTTCATAGCCTT AAA-3′ and NTshRNA-rev 5′-TTTAAGGCTATGAAGAGATAC-3′ as described (Arnette et al., 2016). Keratinocytes were transduced with retroviral supernatants produced from Phoenix cells (provided by G. Nolan, Stanford University, Stanford, CA) in 4 ml of M154 containing the retroviral supernatants and 4 µg/ml of polybrene and incubated at 32°C for 1.5 h followed by two washes of PBS. Fresh media was added and the cultures were returned to 37°C.

siRNA-mediated transfection

After trypsinization, transient transfection of siRNAs into keratinocytes was carried out using 5 µl/ 1.0 × 10^6 cells of human SNAI2 siRNA SMARTpool (Dharmacon, 5′-UCUCUCCUCUUU CCGGAUA-3′, 5′-GCGAUGCCCAGUCUAGAAA-3′, 5′-ACAGCG AACUGGACACACA-3′, 5′-GAAUGUCUCUCCUGCACAA-3′; Catalog No. L-017386-00-0005) or a non-targeting control (Catalog No. D-001206-14-20; Dharmacon) in 100 µl of Ingenio Electroporation Solution (Catalog No. MIR50111; Mirus) using Lonza's Amaxa Nucleofector System, Program X-001. After electroporation, cells were seeded in M154.

Trans-well migration assay

Melanoma cells were pretreated for 24 h with keratinocyte-conditioned media. The following day, 50,000 cells were seeded in 500-µl phenol red-free Opti-MEM in the upper chamber of a 24-well trans-well chamber. DMEM containing 5% FBS was used as a chemoattractant in the lower wells. After 24 h, inner membranes were scrubbed to remove non-migrated cells. Cells on the outer membranes were fixed in formalin and stained with 0.1% crystal violet. Membranes were excised from

the trans-well insert and mounted on glass slides. Migrated cells were visualized by microscopy and counted.

qPCR

Total RNA was extracted from cells using the Quick-RNA miniprep kit (Zymo Research) following the manufacturer's protocol. cDNA was synthesized using 1 µg of RNA using the Superscript III First Strand Synthesis Kit (Thermo Fisher Scientific). Quantitative PCR was performed on the QuantStudio 3 instrument (Thermo Fisher Scientific) using SYBR Green PCR master mix (Thermo Fisher Scientific). Relative mRNA levels were calculated using the ΔΔCT method normalized to GAPDH. Gene specific primers were purchased from Integrated DNA Technologies and sequences are listed as follows: *DSG1*, 5′-TCC ATAGTTGATCGAGAGGTCAC-3′ and 5′-CTGCGTCAGTAGCAT TGCGTA-3′; *DSG3*, 5′-ATCAATGCAACAGATGCAGATGA-3′ and 5′-TGTCAAAGTGTAGCTGCTGTGT-3′; *CDH1*, 5′-GGAAGTCAG TTCAGACTCCAGCC-3′ and 5′-AGGCCTTTTGACTGTAATCAC ACC-3′; *SNAI2*, 5′-ACGCCTCCAAAAAGCCAAA-3′ and 5′-ACT CACTCGCCCCAAAGATG-3′; *GRHL1*, 5′-GGGCATTGATAAGAG AGGCCA-3′ and 5′-ATGGAGTGGGTAGGCATCGT-3′; *CXCL1*, 5′-AACCGAAGTCATAGCCACAC-3′ and 5′-GTTGGATTTGTCACT GTTCAGC-3′; *CXCL2*, 5′-AGATCAATGTGACGGCAGGG-3′ and 5′-TCTCTGCTCTAACACAGAGGGA-3′; *CXCL3*, 5′-CGCCCAAAC CGAAGTCATAG-3′ and 5′-GCTCCCCTTGTTCAGTATCTTTT-3′; *CXCL5*, 5′-AGCTGCGTTGCGTTTGTTTAC-3′ and 5′-TGGCGAACA CTTGCAGATTAC-3′; *CXCL6*, 5′-AGAGCTGCGTTGCACTTGTT-3′ and 5′-GCAGTTTACCAATCGTTTTGGGG-3′; *CXCL7*, 5′-GTAACA GTGCGAGACCACTTC-3′ and 5′-CTTTGCCTTTCGCCAAGTTTC-3′; *CXCL 8*, 5′-ATGACTTCCAAGCTGGCCGT-3′ and 5′-TCCTTG GCAAAACTGCACCT-3′; *IL-6*, 5′-ACAGCCACTCACCTCTTCAG-3′ and 5′-CCATCTTTTTCAGCCATCTTT-3′; and *GAPDH*, 5′-ACC ACAGTCCATGCCATCAC-3′ and 5′-TCCACCACCCTGTTGCTG TA-3′.

Immunofluorescence

For immunostaining, tissue sections were baked at 60°C overnight and deparaffinized using xylenes. Samples were then rehydrated through a series of ethanol and PBS washes. Tissues were permeabilized in 0.5% Triton X-100 in PBS. Antigen retrieval was performed by incubation in 0.01 M citrate buffer at 95°C for 15 min. Sections were blocked in blocking buffer (1% BSA, 2% normal goat serum in PBS) for 60 min at 37°C. Samples were then incubated in primary antibody at 4°C overnight, followed by incubation in secondary antibody for 1 h at 37°C. Images were acquired using an AxioVison Z1 system (Carl Zeiss) with an Apotome slide module, an AxioCam MRm digital camera, and either a 20× (0.8 NA Plan-Apochromat) or 40× (1.4 NA, Plan-Apochromat) oil objective. All images were taken at room temperature at the same exposure and light intensity. Zeiss ZEN software was used for image acquisition. Pixel intensity quantification of staining was carried out in regions of interest (cell borders, nuclei, cytoplasm) using ImageJ software. Keratinocyte staining for Dsg1, Grhl1, and Slug was quantified in keratinocytes directly adjacent to melanoma cells or melanocytes in cultures or patient samples and normalized to staining in keratinocytes two to four cells away from the melanoma cells or melanocytes, in the same layer of the skin if possible. In shDsg1 organotypic cultures, Grhl1 and Slug were quantified in all layers of the epidermis. Grhl1 and Slug staining was quantified as a nuclear to cytoplasmic intensity ratio.

Immunoblot

Whole-cell lysates were collected from confluent monolayers in urea-SDS buffer (8 M urea/1% SDS/60 mM Tris [pH 6.8]/5% ß-mercaptoethanol/10% glycerol) and sonicated. Samples separated by SDS-PAGE were transferred to nitrocellulose, blocked in Odyssey Blocking Buffer (LI-COR Biosciences), and incubated with primary antibodies in blocking buffer overnight at 4°C. After a series of PBS washes, secondary antibodies diluted in blocking buffer at 1:10,000 concentration were added to blots for 1 h at room temperature and then washed with a series of PBS washes. Protein bands were imaged using LI-COR Odyssey FC (LI-COR Biosciences). Densitometric analysis was performed on scanned blots using LI-COR Image Studio software.

RNA sequencing

Differentiated keratinocytes (from three independent primary keratinocyte isolates) were cultured with conditioned media for 48 h and melanoma cells were cultured with conditioned media from keratinocytes (from three independent primary keratinocyte isolates) expressing shNT or shDsg1 for 24 h. Total RNA was extracted from cells using the Quick-RNA miniprep kit (Zymo Research) following the manufacturer's protocol. Novogene Co., LTD conducted preparation of the mRNA library and transcriptome sequencing for two independent runs from identical samples (runs 1 and 2 were processed 1 yr apart at China and Sacramento labs, respectively). Analyses were performed in R (version 4.1.2) using Bioconductor libraries and R statistical packages. Differential expression analysis was performed using DESeq2, with a batch correction to account for keratinocyte clonal variation. Genes with P value < 0.05 and |log2(FoldChange)| > 1 were considered to be differentially expressed. Pathway analysis was performed using Metascape, IPA for Upstream Regulators, and GSEA. Data were deposited in GEO with accession number: GSE239634 (run 2) and https://github.com/NU-AI-SkinBiology/GSE239634_analysis (run 1), and counts and gene names included as Table S1.

Microarray analysis

Microarray analyses of SNAI2 knockdown keratinocytes (GSE55269) were performed in R (version 4.1.2) using Bioconductor libraries and R statistical packages. Affymetrix probe IDs were converted to unique Entrez IDs for analysis and differential expression comparisons were performed using the Limma package.

Statistical analysis

Statistical analysis was performed using GraphPad Prism 8.0 software. All experiments were performed at least three times. Measured data were represented as the mean ± SEM. Data distributions were found to be normal using the Shapiro-Wilk test (for experiments with $n < 8$) or the D'Agostino and Pearson test (for experiments with $n > 8$). One-way analysis of variance

(ANOVA) or two-tail Student's *t* test was applied to compare quantitative data. P values for each analysis are marked on figures and the level of statistical significance was defined as *P < 0.05, **P < 0.01, ***P < 0.001, ****P < 0.0001.

Online supplemental material

Fig. S1 shows GTEx data of Dsg1 expression in sun-exposed and non-sun-exposed skin and the transcriptomics analysis of keratinocytes treated with melanoma-conditioned media. Fig. S2 shows the effects of Dsg1 knockdown on Grhl1 and Slug and confirmation of Grhl1 overexpression. Fig. S3 shows that Slug knockout decreases Dsg1 expression and protein levels and confirmation of knockdown for experiments in Fig. 3. Fig. S4 shows the correlation between Dsg1 knockdown or rescue levels of clones used for conditioned media generation and associated increase in melanoma migration. Fig. S5 shows expression levels of candidate chemokines released by keratinocytes cultured in melanoma-conditioned media. Table S1 includes DESeq2 output for all transcriptomics datasets.

Data availability

Data was deposited in GEO with accession number: GSE239634 (run 2) and https://github.com/NU-AI-SkinBiology/GSE239634_analysis (run 1), and counts and gene names were included as Table S1.

Acknowledgments

The research was supported by the National Institutes of Health (NIH)/National Institute of Arthritis and Musculoskeletal and Skin Diseases (NIAMS) P30 AR075049 awarded to Northwestern University Skin Biology and Diseases Resource-Based Center. Histology services were provided by the Northwestern University Mouse Histology and Phenotyping Laboratory, which is supported by the National Cancer Institute (NCI) P30-CA060553, awarded to the Robert H. Lurie Comprehensive Cancer Center. This work was supported by NIH/NCI R01 CA228196 with additional support from NIH/NIAMS R01 AR041836, NIH/NIAMS R01 AR043380, and the J.L. Mayberry Endowment to K.J. Green. J.L. Pokorny was supported by NIH/NCI T32 CA009560. H.E. Burks was supported by NIH/NCI T32 CA080621-14. Q.R. Roth-Carter was supported by NIH/NCI T32 CA070085. J.T. Seykora was supported by NIH/NIAMS P30-AR069589.

Author contributions: K.J. Green, H.E. Burks, and C.R. Arnette conceived and designed experiments. H.E. Burks, J.L. Koetsier, and J.L. Pokorny acquired data. H.E. Burks, Q.R. Roth-Carter, and J.L. Pokorny performed imaging and data analysis. C.R. Arnette and J.L. Johnson provided training and technical assistance. Z. Ren performed data analysis. P. Gerami and J.T. Seykora provided tissue samples. K.J. Green and H. E. Burks wrote the manuscript.

Disclosures: All authors have completed and submitted the ICMJE Form for Disclosure of Potential Conflicts of Interest. P. Gerami reported personal fees from Castle Biosciences outside the submitted work. No other disclosures were reported.

Submitted: 9 December 2022
Revised: 25 April 2023
Accepted: 16 August 2023

References

Arnette, C., J.L. Koetsier, P. Hoover, S. Getsios, and K.J. Green. 2016. In vitro model of the epidermis: Connecting protein function to 3D structure. *Methods Enzymol.* 569. 287–308. https://doi.org/10.1016/bs.mie.2015.07.015

Arnette, C.R., Q.R. Roth-Carter, J.L. Koetsier, J.A. Broussard, H.E. Burks, K. Cheng, C. Amadi, P. Gerami, J.L. Johnson, and K.J. Green. 2020. Keratinocyte cadherin desmoglein 1 controls melanocyte behavior through paracrine signaling. *Pigment Cell Melanoma Res.* 33:305–317. https://doi.org/10.1111/pcmr.12826

Arnoux, V., M. Nassour, A. L'Helgoualc'h, R.A. Hipskind, and P. Savagner. 2008. Erk5 controls Slug expression and keratinocyte activation during wound healing. *Mol. Biol. Cell.* 19:4738–4749. https://doi.org/10.1091/mbc.e07-10-1078

Brandner, J.M., and N.K. Haass. 2013. Melanoma's connections to the tumour microenvironment. *Pathology*. 45:443–452. https://doi.org/10.1097/PAT.0b013e328363b3bd

Büchau, F., F. Vielmuth, J. Waschke, and T.M. Magin. 2022. Bidirectional regulation of desmosome hyperadhesion by keratin isotypes and desmosomal components. *Cell. Mol. Life Sci.* 79:223. https://doi.org/10.1007/s00018-022-04244-y

Cheng, Y., X.L. Ma, Y.Q. Wei, and X.W. Wei. 2019. Potential roles and targeted therapy of the CXCLs/CXCR2 axis in cancer and inflammatory diseases. *Biochim. Biophys. Acta Rev. Cancer*. 1871:289–312. https://doi.org/10.1016/j.bbcan.2019.01.005

Crowson, A.N., C.M. Magro, and M.C. Mihm Jr. 2006. Prognosticators of melanoma, the melanoma report, and the sentinel lymph node. *Mod. Pathol.* 19:S71–S87. https://doi.org/10.1038/modpathol.3800517

Diener, J., and L. Sommer. 2021. Reemergence of neural crest stem cell-like states in melanoma during disease progression and treatment. *Stem Cells Transl. Med.* 10:522–533. https://doi.org/10.1002/sctm.20-0351

Emert, B.L., C.J. Cote, E.A. Torre, I.P. Dardani, C.L. Jiang, N. Jain, S.M. Shaffer, and A. Raj. 2021. Variability within rare cell states enables multiple paths toward drug resistance. *Nat. Biotechnol.* 39:865–876. https://doi.org/10.1038/s41587-021-00837-3

Galbo, P.M. Jr., X. Zang, and D. Zheng. 2021. Molecular features of cancer-associated fibroblast subtypes and their implication on cancer pathogenesis, prognosis, and immunotherapy resistance. *Clin. Cancer Res.* 27:2636–2647. https://doi.org/10.1158/1078-0432.CCR-20-4226

Getsios, S., E.V. Amargo, R.L. Dusek, K. Ishii, L. Sheu, L.M. Godsel, and K.J. Green. 2004. Coordinated expression of desmoglein 1 and desmocollin 1 regulates intercellular adhesion. *Differentiation*. 72:419–433. https://doi.org/10.1111/j.1432-0436.2004.07208008.x

Getsios, S., C.L. Simpson, S. Kojima, R. Harmon, L.J. Sheu, R.L. Dusek, M. Cornwell, and K.J. Green. 2009. Desmoglein 1-dependent suppression of EGFR signaling promotes epidermal differentiation and morphogenesis. *J. Cell Biol.* 185:1243–1258. https://doi.org/10.1083/jcb.200809044

Godsel, L.M., Q.R. Roth-Carter, J.L. Koetsier, L.C. Tsoi, A.L. Huffine, J.A. Broussard, G.N. Fitz, S.M. Lloyd, J. Kweon, H.E. Burks, et al. 2022. Translational implications of Th17-skewed inflammation due to genetic deficiency of a cadherin stress sensor. *J. Clin. Invest.* 132:e144363. https://doi.org/10.1172/JCI144363

Golan, T., A.R. Messer, A. Amitai-Lange, Z. Melamed, R. Ohana, R.E. Bell, O. Kapitansky, G. Lerman, S. Greenberger, M. Khaled, et al. 2015. Interactions of melanoma cells with distal keratinocytes trigger metastasis via Notch signaling inhibition of MITF. *Mol. Cell*. 59:664–676. https://doi.org/10.1016/j.molcel.2015.06.028

Green, K.J., Q.R. Roth-Carter, C.M. Niessen, and S.A. Nichols. 2020. Tracing the origins of the desmosome: A vertebrate innovation. *Curr. Biol.* 30:R535–R543. https://doi.org/10.1016/j.cub.2020.03.047

Haass, N.K., K.S. Smalley, L. Li, and M. Herlyn. 2005. Adhesion, migration and communication in melanocytes and melanoma. *Pigment Cell Res.* 18:150–159. https://doi.org/10.1111/j.1600-0749.2005.00235.x

Harmon, R.M., C.L. Simpson, J.L. Johnson, J.L. Koetsier, A.D. Dubash, N.A. Najor, O. Sarig, E. Sprecher, and K.J. Green. 2013. Desmoglein-1/Erbin interaction suppresses ERK activation to support epidermal differentiation. *J. Clin. Invest.* 123:1556–1570. https://doi.org/10.1172/JCI65220

Hegazy, M., A.L. Perl, S.A. Svoboda, and K.J. Green. 2022. Desmosomal cadherins in health and disease. *Annu. Rev. Pathol.* 17:47–72. https://doi.org/10.1146/annurev-pathol-042320-092912

Hsu, M.Y., F.E. Meier, M. Nesbit, J.Y. Hsu, P. Van Belle, D.E. Elder, and M. Herlyn. 2000. E-cadherin expression in melanoma cells restores keratinocyte-mediated growth control and down-regulates expression of invasion-related adhesion receptors. *Am. J. Pathol.* 156:1515–1525. https://doi.org/10.1016/S0002-9440(10)65023-7

Johnson, J.L., J.L. Koetsier, A. Sirico, A.T. Agidi, D. Antonini, C. Missero, and K.J. Green. 2014. The desmosomal protein desmoglein 1 aids recovery of epidermal differentiation after acute UV light exposure. *J. Invest. Dermatol.* 134:2154–2162. https://doi.org/10.1038/jid.2014.124

Kalaora, S., A. Nagler, J.A. Wargo, and Y. Samuels. 2022. Mechanisms of immune activation and regulation: Lessons from melanoma. *Nat. Rev. Cancer*. 22:195–207. https://doi.org/10.1038/s41568-022-00442-9

Kowalczyk, A.P., and K.J. Green. 2013. Structure, function, and regulation of desmosomes. *Prog. Mol. Biol. Transl. Sci.* 116:95–118. https://doi.org/10.1016/B978-0-12-394311-8.00005-4

Mescher, M., P. Jeong, S.K. Knapp, M. Rübsam, M. Saynisch, M. Kranen, J. Landsberg, M. Schlaak, C. Mauch, T. Tüting, et al. 2017. The epidermal polarity protein Par3 is a non-cell autonomous suppressor of malignant melanoma. *J. Exp. Med.* 214:339–358. https://doi.org/10.1084/jem.20160596

Miao, Y., W. Zhang, S. Liu, X. Leng, C. Hu, and H. Sun. 2021. HOXC10 promotes growth and migration of melanoma by regulating Slug to activate the YAP/TAZ signaling pathway. *Discov. Oncol.* 12:12. https://doi.org/10.1007/s12672-021-00408-7

Mistry, D.S., Y. Chen, Y. Wang, K. Zhang, and G.L. Sen. 2014. SNAI2 controls the undifferentiated state of human epidermal progenitor cells. *Stem Cells*. 32:3209–3218. https://doi.org/10.1002/stem.1809

Molina-Ortiz, I., R.A. Bartolomé, P. Hernández-Varas, G.P. Colo, and J. Teixidó. 2009. Overexpression of E-cadherin on melanoma cells inhibits chemokine-promoted invasion involving p190RhoGAP/p120ctn-dependent inactivation of RhoA. *J. Biol. Chem.* 284:15147–15157. https://doi.org/10.1074/jbc.M807834200

Polivka, L., S. Hadj-Rabia, E. Bal, S. Leclerc-Mercier, M. Madrange, Y. Hamel, D. Bonnet, S. Mallet, H. Lepidi, C. Ovaert, et al. 2018. Epithelial barrier dysfunction in desmoglein-1 deficiency. *J. Allergy Clin. Immunol.* 142:702–706.e7. https://doi.org/10.1016/j.jaci.2018.04.007

Roth-Carter, Q.R., J.L. Koetsier, J.A. Broussard, and K.J. Green. 2022. Organotypic human skin cultures incorporating primary melanocytes. *Curr. Protoc.* 2:e536. https://doi.org/10.1002/cpz1.536

Samuelov, L., O. Sarig, R.M. Harmon, D. Rapaport, A. Ishida-Yamamoto, O. Isakov, J.L. Koetsier, A. Gat, I. Goldberg, R. Bergman, et al. 2013. Desmoglein 1 deficiency results in severe dermatitis, multiple allergies and metabolic wasting. *Nat. Genet.* 45:1244–1248. https://doi.org/10.1038/ng.2739

Schweppe, R.E., T.H. Cheung, and N.G. Ahn. 2006. Global gene expression analysis of ERK5 and ERK1/2 signaling reveals a role for HIF-1 in ERK5-mediated responses. *J. Biol. Chem.* 281:20993–21003. https://doi.org/10.1074/jbc.M604208200

Shaffer, S.M., M.C. Dunagin, S.R. Torborg, E.A. Torre, B. Emert, C. Krepler, M. Beqiri, K. Sproesser, P.A. Brafford, M. Xiao, et al. 2017. Rare cell variability and drug-induced reprogramming as a mode of cancer drug resistance. *Nature*. 546:431–435. https://doi.org/10.1038/nature22794

Shain, A.H., N.M. Joseph, R. Yu, J. Benhamida, S. Liu, T. Prow, B. Ruben, J. North, L. Pincus, I. Yeh, et al. 2018. Genomic and transcriptomic analysis reveals incremental disruption of key signaling pathways during melanoma evolution. *Cancer Cell*. 34:45–55.e4. https://doi.org/10.1016/j.ccell.2018.06.005

Sharma, B., S. Singh, M.L. Varney, and R.K. Singh. 2010. Targeting CXCR1/CXCR2 receptor antagonism in malignant melanoma. *Expert Opin. Ther. Targets*. 14:435–442. https://doi.org/10.1517/14728221003652471

Shirley, S.H., V.R. Greene, L.M. Duncan, C.A. Torres Cabala, E.A. Grimm, and D.F. Kusewitt. 2012. Slug expression during melanoma progression. *Am. J. Pathol.* 180:2479–2489. https://doi.org/10.1016/j.ajpath.2012.02.014

Simpson, C.L., S. Kojima, and S. Getsios. 2010. RNA interference in keratinocytes and an organotypic model of human epidermis. *Methods Mol. Biol.* 585:127–146. https://doi.org/10.1007/978-1-60761-380-0_10

Singh, S., K.C. Nannuru, A. Sadanandam, M.L. Varney, and R.K. Singh. 2009. CXCR1 and CXCR2 enhances human melanoma tumourigenesis, growth and invasion. *Br. J. Cancer*. 100:1638–1646. https://doi.org/10.1038/sj.bjc.6605055

Siret, C., C. Terciolo, A. Dobric, M.C. Habib, S. Germain, R. Bonnier, D. Lombardo, V. Rigot, and F. André. 2015. Interplay between cadherins and α2β1 integrin differentially regulates melanoma cell invasion. *Br. J. Cancer*. 113:1445–1453. https://doi.org/10.1038/bjc.2015.358

Tang, K.H., S. Ma, T.K. Lee, Y.P. Chan, P.S. Kwan, C.M. Tong, I.O. Ng, K. Man, K.F. To, P.B. Lai, et al. 2012. CD133(+) liver tumor-initiating cells promote tumor angiogenesis, growth, and self-renewal through neurotensin/interleukin-8/CXCL1 signaling. *Hepatology*. 55:807–820. https://doi.org/10.1002/hep.24739

Thaper, D., S. Vahid, K.M. Nip, I. Moskalev, X. Shan, S. Frees, M.E. Roberts, K. Ketola, K.W. Harder, C. Gregory-Evans, et al. 2017. Targeting Lyn regulates Snail family shuttling and inhibits metastasis. *Oncogene*. 36:3964–3975. https://doi.org/10.1038/onc.2017.5

Tsoi, J., L. Robert, K. Paraiso, C. Galvan, K.M. Sheu, J. Lay, D.J.L. Wong, M. Atefi, R. Shirazi, X. Wang, et al. 2018. Multi-stage differentiation defines melanoma subtypes with differential vulnerability to drug-induced iron-dependent oxidative stress. *Cancer Cell*. 33:890–904.e5. https://doi.org/10.1016/j.ccell.2018.03.017

Upadhyay, P.R., T. Ho, and Z.A. Abdel-Malek. 2021. Participation of keratinocyte- and fibroblast-derived factors in melanocyte homeostasis, the response to UV, and pigmentary disorders. *Pigment Cell Melanoma Res.* 34:762–776. https://doi.org/10.1111/pcmr.12985

Vandyck, H.H., L.M. Hillen, F.M. Bosisio, J. van den Oord, A. Zur Hausen, and V. Winnepenninckx. 2021. Rethinking the biology of metastatic melanoma: A holistic approach. *Cancer Metastasis Rev.* 40:603–624. https://doi.org/10.1007/s10555-021-09960-8

Villanueva, J., and M. Herlyn. 2008. Melanoma and the tumor microenvironment. *Curr. Oncol. Rep.* 10:439–446. https://doi.org/10.1007/s11912-008-0067-y

Wang, J.X., M. Fukunaga-Kalabis, and M. Herlyn. 2016. Crosstalk in skin: Melanocytes, keratinocytes, stem cells, and melanoma. *J. Cell Commun. Signal.* 10:191–196. https://doi.org/10.1007/s12079-016-0349-3

Wang, S., M.L. Drummond, C.F. Guerrero-Juarez, E. Tarapore, A.L. MacLean, A.R. Stabell, S.C. Wu, G. Gutierrez, B.T. That, C.A. Benavente, et al. 2020. Single cell transcriptomics of human epidermis identifies basal stem cell transition states. *Nat. Commun.* 11:4239. https://doi.org/10.1038/s41467-020-18075-7

Wessely, A., T. Steeb, C. Berking, and M.V. Heppt. 2021. How neural crest transcription factors contribute to melanoma heterogeneity, cellular plasticity, and treatment resistance. *Int. J. Mol. Sci.* 22:5761. https://doi.org/10.3390/ijms22115761

Wilanowski, T., J. Caddy, S.B. Ting, N.R. Hislop, L. Cerruti, A. Auden, L.L. Zhao, S. Asquith, S. Ellis, R. Sinclair, et al. 2008. Perturbed desmosomal cadherin expression in grainy head-like 1-null mice. *EMBO J.* 27:886–897. https://doi.org/10.1038/emboj.2008.24

Yao, D., C. Li, M.S.R. Rajoka, Z. He, J. Huang, J. Wang, and J. Zhang. 2020. P21-Activated Kinase 1: Emerging biological functions and potential therapeutic targets in Cancer. *Theranostics*. 10:9741–9766. https://doi.org/10.7150/thno.46913

Yardman-Frank, J.M., and D.E. Fisher. 2021. Skin pigmentation and its control: From ultraviolet radiation to stem cells. *Exp. Dermatol.* 30:560–571. https://doi.org/10.1111/exd.14260

Supplemental material

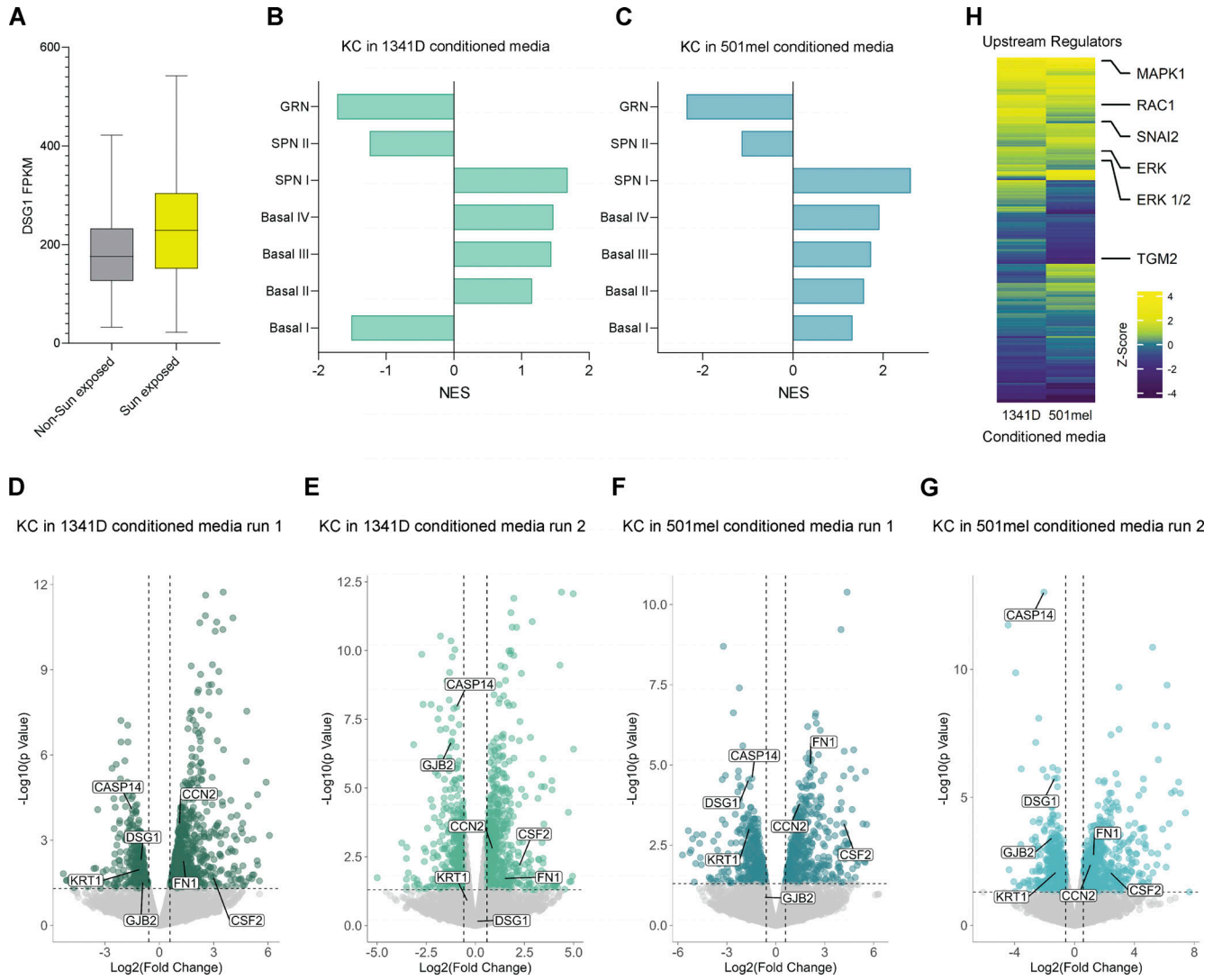

Figure S1. **Dsg1 expression in sun-exposed and non-sun-exposed skin; transcriptomic analysis reveals increased activation of keratinocyte Slug and reduced keratinocyte differentiation signaling by melanoma cells. (A)** GTEx (Genotype-Tissue Expression) data showing Dsg1 mRNA levels were not altered in chronically sun-exposed skin. FPKM, bars represent minimum and maximum values. **(B and C)** Gene set enrichment analysis (GSEA) of RNA Seq run 2 comparing differentially expressed gene sets to published signatures of primary human keratinocyte differentiation expression patterns show a decrease in the enrichment of granular (GRN) and spinous II (SPNII) layer genes. **(D–G)** mRNA sequencing was performed on primary human keratinocytes (KC) treated with conditioned media from melanocytes or melanoma cells. Volcano plots depict significantly changed genes in keratinocytes treated with melanoma-conditioned media compared with those treated with melanocyte-conditioned media. Highlighted genes are those involved in pathways of differentiation and the identified upstream regulators for keratinocytes treated with 1341D media (run 1, D; run 2, E) or 501mel conditioned media (run 1, F; run 2, G). **(H)** Heatmap showing upstream regulators in keratinocytes predicted to be activated by melanoma conditioned media (run 2) using Ingenuity Pathway Analysis (IPA) including RAC1, Snai2, and MAPK family signaling members.

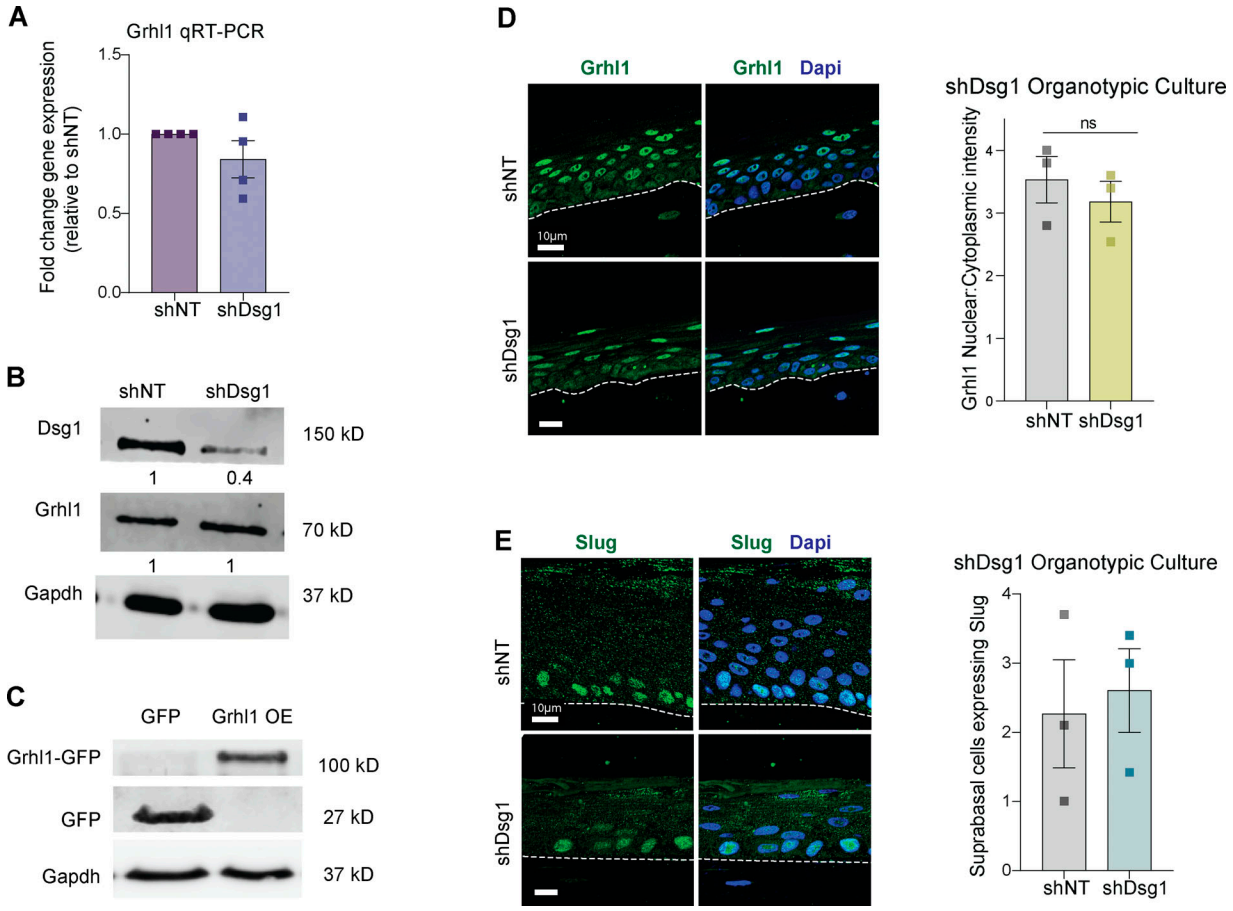

Figure S2. **Grhl1 is regulated upstream of Dsg1. (A and B)** Retroviral transduction of shNT (non-targeting control) or shDsg1 knockdown vectors was performed in primary human keratinocytes and RNA or protein was collected for RT-PCR and Western blot validation of knockdown. No significant difference in Grhl1 mRNA expression or protein level was observed in response to Dsg1 knockdown. **(C)** Retroviral transduction of GFP or GRHL1 (Grhl1 OE) was performed in primary human keratinocytes and protein was collected for Western blot validation of expression (see Fig. 3 H). **(D)** 3D organotypic raft cultures comprises shNT or shDsg1 expressing keratinocytes were grown for 6 d and stained for Grhl1. Nuclear to cytoplasmic staining intensity of Grhl1 was not statistically different between the two cultures. Mean ± SEM depicted. $n = 3$, Student's t test. **(E)** Similarly, 3D organotypic raft cultures composed of shNT or shDsg1 expressing keratinocytes were grown for 6 d and stained for Slug and the number of suprabasal Slug expressing cells was counted. The number of suprabasal Slug expressing cells was not different between the two cultures. $n = 3$. Student's t test. Source data are available for this figure: SourceData FS2.

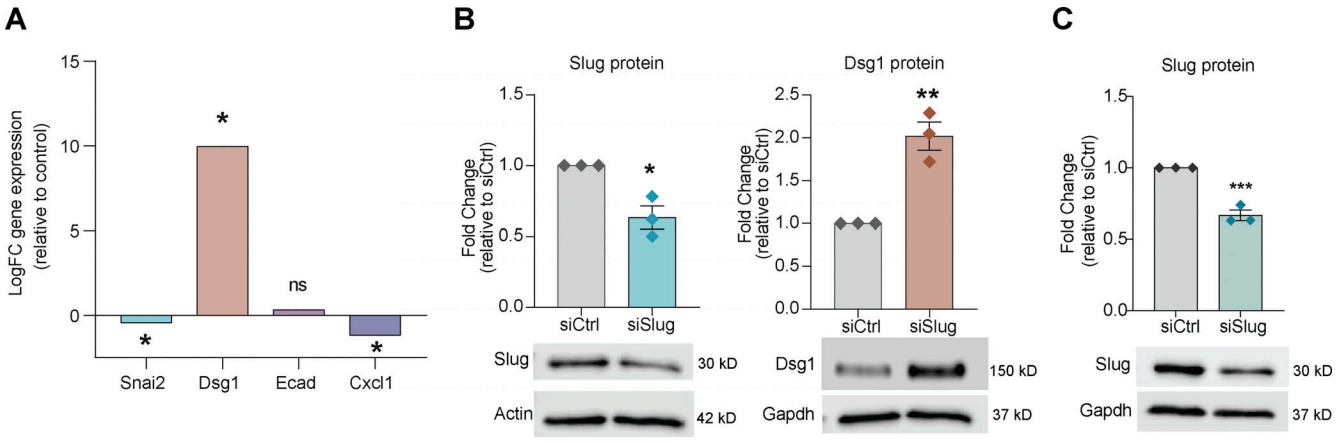

Figure S3. **Slug loss in keratinocytes results in decreased Dsg1. (A)** Microarray data shows an increase in Dsg1 expression in primary human keratinocytes upon loss of Slug expression, as well as a concurrent decrease in CXCL1 expression. **(B)** siRNA knockdown of Slug causes an increase in Dsg1 protein levels as seen by Western blot. $n = 3$. *P < 0.05, **P < 0.01. Student's t test. **(C)** Slug knockdown levels assessed by Western blot, corresponding to experiment in Fig. 3, I and J. Source data are available for this figure: SourceData FS3.

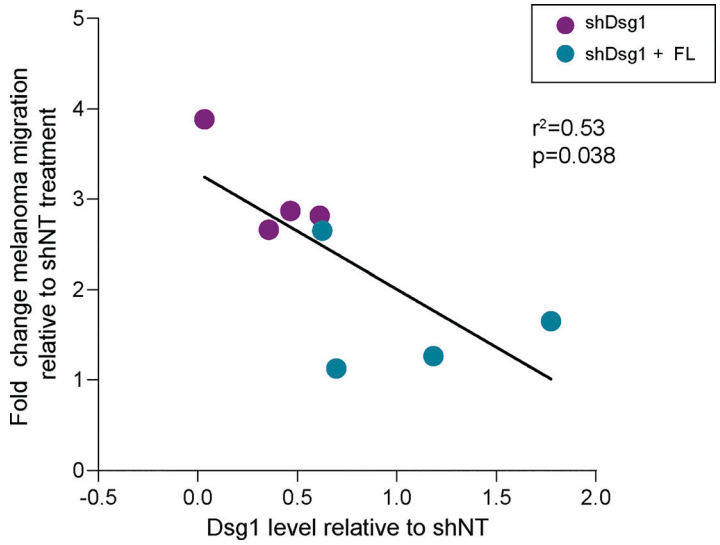

Figure S4. **Modulation of melanoma migration is correlated with Dsg1 levels in keratinocytes.** Conditioned media from primary keratinocytes derived from four separate donors was used to treat melanoma cells in migration assays. Dsg1 knockdown and rescue were not equal in each clone. Shown is a graph of the average migration increase in melanoma cells upon treatment with shDsg1 conditioned media or shDsg1 + FL conditioned media compared with control, correlated with the keratinocyte Dsg1 protein levels in the clones used for each in the shDsg1 cells (purple) and the shDsg1 + FL cells (blue).

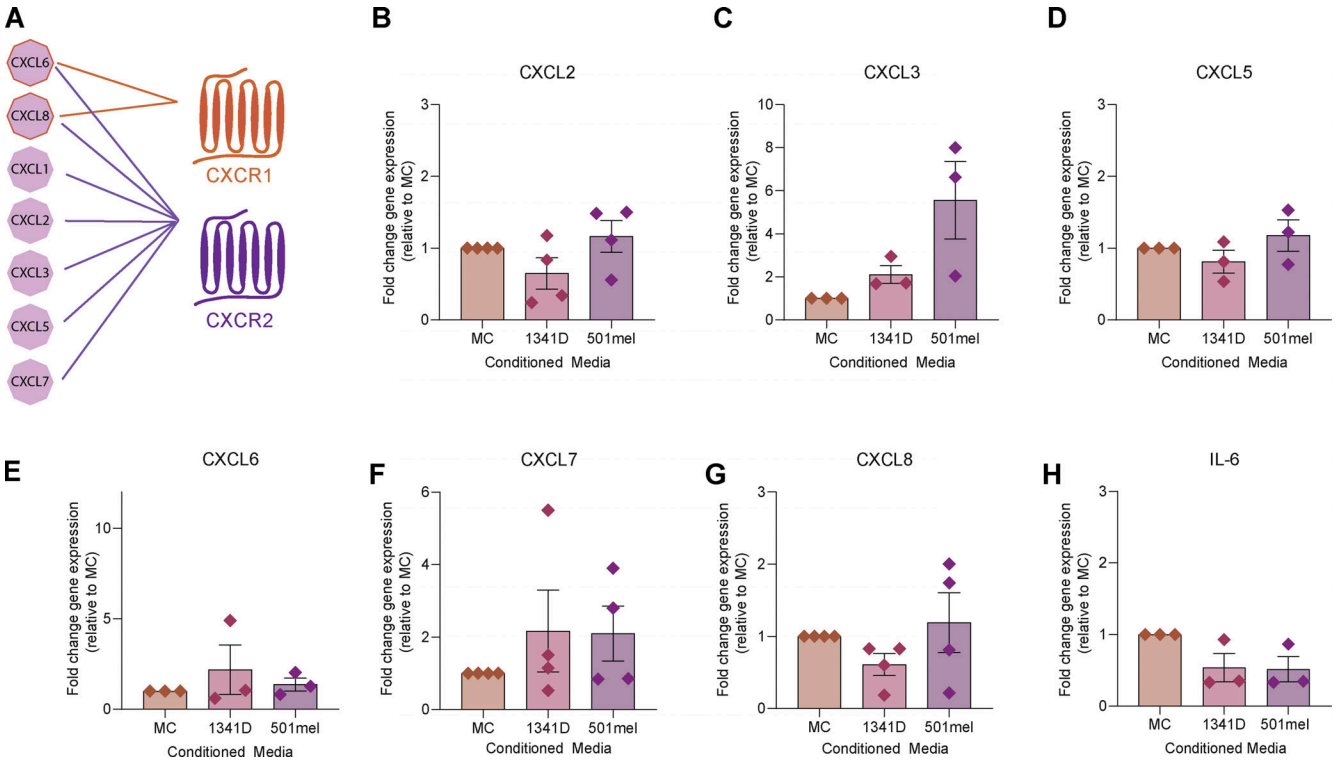

Figure S5. **Gene expression of candidate keratinocyte chemokines and cytokines released in response to melanoma-conditioned media. (A)** Schematic depicting receptor-ligand binding partners for candidate chemokine targets. **(B–H)** Primary human keratinocytes were treated for 48 h with conditioned media from melanocytes (MC) or the melanoma cell lines WM1341D and 501mel and RNA was collected. RT-PCR was performed for chemokines and cytokines induced by shDsg1. Mean ± SEM depicted. *n* = 3. One-way ANOVA.

Provided online is Table S1. Table S1 shows DESeq2 output for all transcriptomics datasets used in this study.